



The Sync-Fire/deSync model: Modelling the reactivation of dynamic memories from cortical alpha oscillations

George Parish^{a,*}, Sebastian Michelmann^b, Simon Hanslmayr^c, Howard Bowman^{a,d}

^a School of Psychology and Centre for Human Brain Health, University of Birmingham, UK

^b Department of Psychology, Princeton University, USA

^c Institute of Neuroscience and Psychology & Centre for Cognitive Neuroimaging, University of Glasgow, UK

^d School of Computing, University of Kent, UK

ARTICLE INFO

Keywords:

Brain oscillations
Episodic memory model
Attentional blink
Temporal sequence model

ABSTRACT

We propose a neural network model to explore how humans can learn and accurately retrieve temporal sequences, such as melodies, movies, or other dynamic content. We identify target memories by their neural oscillatory signatures, as shown in recent human episodic memory paradigms. Our model comprises three plausible components for the binding of temporal content, where each component imposes unique limitations on the encoding and representation of that content. A cortical component actively represents sequences through the disruption of an intrinsically generated alpha rhythm, where a desynchronisation marks information-rich operations as the literature predicts. A binding component converts each event into a discrete index, enabling repetitions through a sparse encoding of events. A timing component – consisting of an oscillatory “ticking clock” made up of hierarchical synfire chains – discretely indexes a moment in time. By encoding the absolute timing between discretised events, we show how one can use cortical desynchronisations to dynamically detect unique temporal signatures as they are reactivated in the brain. We validate this model by simulating a series of events where sequences are uniquely identifiable by analysing phasic information, as several recent EEG/MEG studies have shown. As such, we show how one can encode and retrieve complete episodic memories where the quality of such memories is modulated by the following: alpha gate keepers to content representation; binding limitations that induce a blink in temporal perception; and nested oscillations that provide preferential learning phases in order to temporally sequence events.

1. Introduction

When we remember detailed episodic memories, we often do this in a temporally accurate way (e.g. when we hum a melody that we only heard once). This implies that our brain has the ability to represent temporally accurate patterns as they unfold over time. Through extensive electroencephalography (EEG) & magnetoencephalography (MEG) recordings, we have been able to identify the neural oscillations that are thought to implement such functionality, in particular, during learning (Buzsáki, 2002; Fell and Axmacher, 2011) and information processing (Hanslmayr et al., 2012; Jensen and Mazaheri, 2010; Klimesch et al., 2007). Here, it has been proposed that oscillations provide shared up-states that enable precise communication between disparate neural populations (Fries, 2005). A candidate mechanism for the regulation of such information processing are brain oscillations in the alpha band

(8–12Hz). Such rhythmic oscillations are thought to provide a gating function to the representation of information (Jensen and Mazaheri, 2010; Klimesch et al., 2007), where information representation would be measurable by oscillatory power changes in specific frequencies. As such, alpha frequency de-synchronisations are thought to signify information processing in cortical regions, as de-regulated neural activation enables potential information gain (Hanslmayr et al., 2012). Evidence has also been provided that successful episodic memory encoding and retrieval can be predicted by alpha power decreases (i.e. de-synchronisations) in several experimental (Fell et al., 2011; Hanslmayr and Staudigl, 2014; Khader et al., 2010; Klimesch et al., 2005; Waldhauser et al., 2016), and modelling (Parish et al., 2018) studies.

Importantly, the timing of activation relative to this intrinsic rhythm generator is key (Canaviev, 2015). A form of representational similarity analysis (RSA; see Equation (16) of the Appendix), that involves

* Corresponding author.

E-mail address: g.parish@bham.ac.uk (G. Parish).

<https://doi.org/10.1016/j.neuropsychologia.2021.107867>

Received 28 August 2020; Received in revised form 19 April 2021; Accepted 20 April 2021

Available online 24 April 2021

0028-3932/© 2021 The Authors. Published by Elsevier Ltd. This is an open access article under the CC BY license (<http://creativecommons.org/licenses/by/4.0/>).

convolving one pattern across another to detect similarity, has recently been employed to detect the active representation of neural patterns at encoding (Ng et al., 2013; Schyns et al., 2011) and retrieval (Staresina et al., 2016; Staudigl et al., 2015; Wimber et al., 2012; Yaffe et al., 2014). In this way, it is thought that the active representation of information breaks the rhythmicity of an entraining oscillation by resetting its intrinsic phase relative to some input (Canavier, 2015), enabling stimuli of interest to stand out from the surrounding rhythmicity of the brain (Hanslmayr et al., 2012). Consecutive phase-resets such as these, have been found to form a temporal signature that uniquely identifies specific sequences, allowing detection of the reactivation of visual or auditory stimuli (Staudigl and Hanslmayr, 2019), replay of complex movie sequences (Michelmann et al., 2019), reactivation in working memory (Michelmann et al., 2018) and episodic memory (Michelmann et al., 2016), and even reactivation during sleep (Schreiner et al., 2018). More broadly, a number of recent MEG studies leveraged other multivariate analysis methods to detect reactivation of sequences (Kornysheva et al., 2019; Kurth-Nelson et al., 2016; Lui et al., 2019).

In addition to the alpha band, which is thought to regulate information representation in a decipherable manner (Hanslmayr et al., 2012; Michelmann et al., 2016), an oscillatory hierarchy also seems to be important for stimulus processing (Lakatos et al., 2005). These occur when the phase of slower oscillations modulates the amplitude of faster oscillations, typically in a hierarchy of delta (1–4Hz), theta (4–8Hz) & gamma (30–50Hz) frequencies. It is thought that the synchronisation of these nested EEG oscillations enables attentional (Lakatos et al., 2008) and sensory (Schroeder and Lakatos, 2009) selection, by providing a temporal reference frame for visual (Barczak et al., 2019) and auditory (Tai et al., 2020) processing.

In light of these findings, there is a substantial lack of theoretical work that explores the functional role that such oscillations might play in information processing and human episodic memory. As such, we aim here to model the memory-reinstatement of temporal patterns in the cortex, in a way that is physiologically plausible and consistent with empirical findings. The respective code can be found here (<https://github.com/GP2789/The-Sync-fire-deSync-Model>). Here, we focus on the dichotomy of oscillatory synchronisation, and its functional role for human episodic memory (Hanslmayr et al., 2016). As in previous modelling work (Parish et al., 2018), we build on the notion that low frequency desynchronisation in the alpha/beta frequency range (8–25Hz) is indicative of the active representation of information (Hanslmayr et al., 2012), which we further decode here to decipher information content (Michelmann et al., 2016). Previously (Parish et al., 2018), we explored the notion that hippocampal theta synchronisation provides phases of optimal learning (Hasselmo et al., 2002; Huerta and Lisman, 1995; Pavlides et al., 1988). Here, we model a potential neural substrate for hierarchical frequency coupling, which is thought to promote stimulus (Lakatos et al., 2005), sensory (Schroeder and Lakatos, 2009) & attentional (Lakatos et al., 2008) selectivity. Previous modelling work has suggested that such a nested hierarchy of oscillators might play a role in maintaining an ordinal sequence in working memory (Jensen et al., 1996), where successive items are stored in successive gamma slots within a theta cycle (Lisman and Jensen, 2013). We here explore the notion that these intrinsic hierarchical oscillators might more generally imbue the brain with the capability to encode the beats of human episodic memory, providing temporal reference points for the encoding of information, as is thought to occur in auditory (Tai et al., 2020) and visual (Barczak et al., 2019) processing.

We here take inspiration from previous modelling work on the notion of time-keeping in the brain (Itskov et al., 2011; Rolls and Mills, 2019; Shankar and Howard, 2012), though the focus of these works has typically not been to demonstrate the ability to encode and retrieve temporally reliable content. As such, our primary motivation here is to explore the necessary ingredients for a neuro-physiologically plausible framework, grounded by experimental findings, to encode and retrieve identifiable episodic memories. The current modelling work is a

continuation of the Sync/deSync hypothesis (Hanslmayr et al., 2016; Parish et al., 2018). Oscillatory synchronisations are thought to mediate communication (Fries, 2005), processing (Lakatos et al., 2005) & learning (Fell and Axmacher, 2011; Hasselmo et al., 2002), whilst also acting to control cortical excitability (Klimesch et al., 2007). In this way a desynchronisation represents information flow (Hanslmayr et al., 2012) that can be decoded (Michelmann et al., 2016).

We achieve the encoding and retrieving of episodic content by implementing a complementary learning systems (CLS) framework (McClelland et al., 1995), where the encoding of content is facilitated by a plastic hippocampal region, and the storage and representation of that content is enabled by a stable cortical region. We simulate three interacting neural assemblies that together enable the encoding and reactivation of episodic memories. We show that our model can learn and retrieve temporally dynamic episodes and that these episodes become identifiable via their temporal pattern of activity, which is accompanied by power decreases in the alpha band. This model implements recent theoretical considerations about the role of alpha (Hanslmayr et al., 2012; Klimesch et al., 2007) and other nested frequencies (Lakatos et al., 2005). We reproduce several empirical findings that show content specific reactivation of temporal patterns in the alpha band (Michelmann et al., 2016), enabling us to make predictions as to how the quality of episodic content can be affected by oscillatory modulation and binding processes.

2. Model architecture

The following modelling work is intended as a proof of concept, exploring a plausible theoretical position as to how the encoding and retrieval of a temporally accurate memory might be achieved in the human brain. This allows us to explore the validity of several hypotheses made by contemporary empirical studies. Specifically, two hypotheses are that jumps in the phase of the intrinsic alpha oscillation can be “read” by a higher function (or external observer) to consistently identify unique memory traces (Michelmann et al., 2016) and that nested frequency bands might contextualise episodic memories by providing temporal reference frames (Tai et al., 2020). By exploring such phenomena in a theoretical model, we go on to show how oscillations might enhance the episodic distinctiveness of memories, that is, by providing oscillatory blind spots that act to segregate temporal episodes into discernible chunks, maximising temporal context and minimising binding errors.

To achieve these goals, our modelling works with interacting populations of single cells in an abstract manner. Though single cells are modelled in depth to allow us to accurately capture the phasic and plastic properties of a population, populations do not directly map onto any given neurophysiological counterpart – though their functions are inspired by them. Similarly, the scope of our analyses is limited to small target memories of just a few stimuli over a short period of time. Our primary motivation being to investigate the limitations of our entire theoretical structure with respect to both representing and binding information, rather than the potential storage capacity or versatility in forward or backward replay of episodic sequences. Once encoded, temporal memories are reactivated by reversing the pathway of activation with no concern for the context of the retrieval, such as time delays, wakefulness or sleep stage, etc. Our primary consideration in this matter is the strengthening of target synapses through co-activation under a Hebbian approach, allowing for the accurate reactivation of temporally organised content that can be identified through contemporary analytical means, such as RSA.

As the purpose of this model is to explore a theoretical position concerning the accurate encoding and reactivation of temporally organised content, we here put forward several hypotheses as to the components that seem necessary to fulfil this objective. Primarily, we are theorising that there might exist some form of stable, non-plastic timekeeper that maintains a sequential order of unique temporal

positions. We argue that this is an important concept for not only remembering the sequential order of beats in a rhythm, but also the temporal lag between them. In doing so, we put forward that a hierarchical oscillatory solution would be the most cost-effective and robust. Additionally, if our two primary ingredients in the formation of memories are the co-activation of dynamic content and temporal position, we also consider that there might be a discrete binding region that abstractly glues these two elements together. The purpose of this region would be to create a unique identifiable index for each temporally consecutive element in an episodic memory trace, such as a content shift or scene change, which unifies all sensory elements of the content under a single abstract label. We can also show that an attentional deficit is induced for content shifts that occur very close together in time, aligning our model with the well explored attentional-blink phenomenon (Bowman and Wyble, 2007; Swan and Wyble, 2014; Wyble et al., 2011;

Raymond et al., 1992; Chun and Potter, 1995).

As one of the first neurophysiological models to foray into the encoding, reactivation & detection of whole human episodic memories, we hope to stimulate alternative theoretical frameworks to tackle this issue in a way that is also consistent with empirical studies.

Previous modelling work (Parish et al., 2018) explored how alpha power decreases could be due to the active processing of stimuli (Hanslmayr et al., 2012), which entails alpha acting as an inhibitory gate-keeper to the representation of cortically stored information (Klimesch et al., 2007) in a CLS framework (O'Reilly et al., 2011). Such a framework considers the proposition that catastrophic forgetting is an ever-present danger when learning occurs in a single system framework (McCloskey and Cohen, 1989), proposing instead that two complementary systems are better suited to encode new memories and store old memories, respectively (McClelland et al., 1995). As in other models

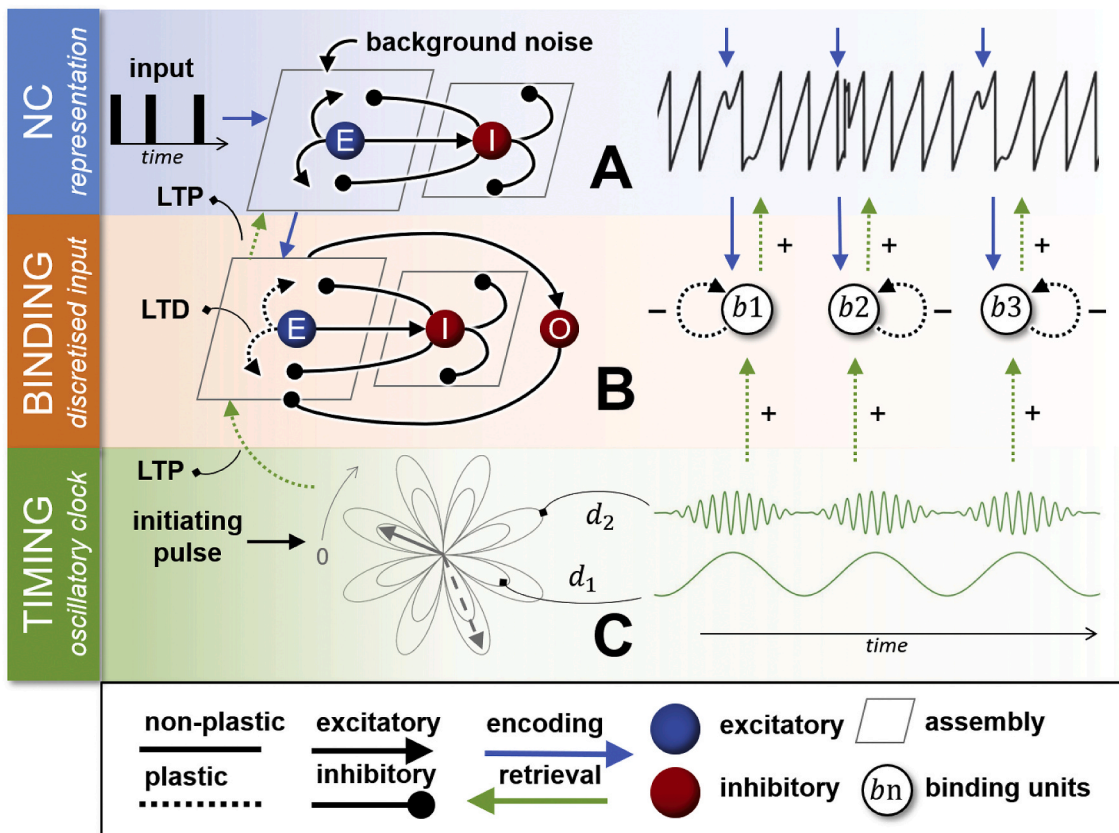


Fig. 1. Architecture of a spiking neural network model, using Hodgkin-Huxley equations (Hodgkin and Huxley, 1952). A neo-cortical (NC) region comprised of recurrent excitatory-inhibitory interactions, intrinsically oscillates through the reception of low-level (non-oscillatory) background noise (A, left-hand section: blue excitatory population & red inhibitory population). “Winner-take-all” behaviour was encouraged by short-range excitatory and long-range inhibitory connections, enabling the clear representation of each input. During encoding (blue top-down arrows), a sequence of incoming cortical stimuli trigger activation in a binding pool (B, left-hand section: blue excitatory population, red inhibitory population & additional red inhibitory “off-switch” node), a broadly tuned population that indexes each stimulus as a unique event through a combination of long-term potentiation (LTP) and hetero-synaptic long-term depression (LTD). An additional inhibitory node was required to prevent runaway excitation, what we term an “off-switch”. Through LTP, active binding assemblies form a direct connection between concurrently active hierarchical synfire chains (C, left-hand section: a feed-forward & clock-like structure used for the encoding of time, described in Figs. 2 and 3), and the NC representation of the stimulus. Conversely, LTD occurs within active binding pool assemblies, diminishing the likelihood that they would be able to compete for the indexing of subsequent stimuli. This is a form of hetero-synaptic LTD in response to the LTP occurring on other dendrites (Volgushev et al., 2016). Altogether, binding pool LTP & LTD ensures a sparse coding to index unique events. During recall (green bottom-up arrows), synfire chains are re-started and the relevant bindings are activated in sequence until the original pattern is re-instantiated in representational regions. Visualising this process through time in the right-hand sections of A-C, observable phase-reset patterns emerge in the intrinsically oscillating cortical region to represent information content (A, right-hand section: blue top-down arrows indicate the occurrence of stimuli and subsequent phase-resets). Describing the top-down encoding state, a sparse coding then indexes events in the binding pool region (B, right-hand section; numbered nodes indicate the occurrence of a unique binding assembly), which are bound to the ticking hierarchical oscillator (C, right-hand section: nested oscillatory frequencies). This enables events to be bound relative to a temporal rhythm (blue top-down arrows), ensuring that they can be recalled (green bottom-up arrows) with the correct absolute timing between events. We assume the presence of a neuro-modulator that switches information processing between the encoding direction (blue top-down arrows) and the retrieval direction (green bottom-up arrows), which is important to prevent cross-communication from contaminating encoding and recall processes. This is achieved by setting the weights of each pathway to zero at the appropriate processing phase. See the supplementary materials for more information on topology and parameter definitions.

(O'Reilly et al., 2011), we here instantiate a cortical region where long-term memories can be stored and safely reactivated without the risk of catastrophic interference (see Fig. 1A). We build on our previous modelling work (Parish et al., 2018) by further exploring the relation of information processing to a simulated alpha rhythm. In our previous implementation of cortical alpha as an *extrinsic* constant frequency, we showed how a gradual increase in stimulus strength overcomes inhibition, at first synchronising and strengthening the entraining oscillation, until input succeeds in desynchronising the rhythm to actively represent the stimulus in question. In our current implementation of cortical alpha as an *intrinsically* oscillating neural assembly, we show how the timing of

a stimulus is as important as its strength in predicting whether the stimulus will trigger a desynchronising phase-reset, or be lost in the entraining rhythm. As such, we explore a cortical oscillatory mechanism that enables information to be represented with respect to the surrounding rhythmicity of the brain.

When taken together with the implication of nested rhythmic pacemakers in stimulus processing (Lakatos et al., 2005; Barczak et al., 2019; Tai et al., 2020), we here show how human episodic memories might be formed by desynchronised content being bound together relative to synchronised time-keeping oscillators (see Fig. 1C). This binding process makes up the other half of our CLS framework (O'Reilly et al., 2011),

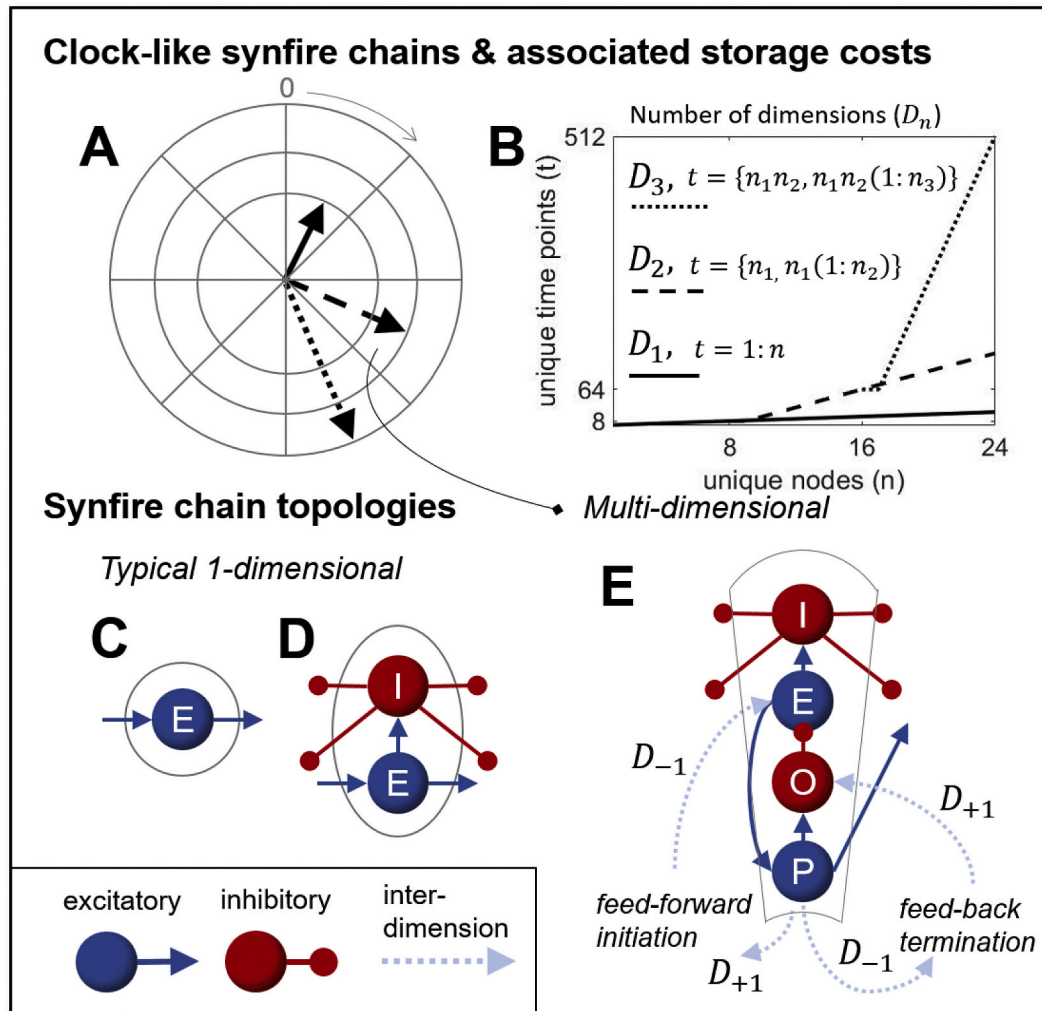


Fig. 2. Considering the storage cost of using multi-dimensional synfire chains in the representation of time (A). In B, we show how the required storage for the use of synfire chains in representing a given set of unique time points decreases as one increases the dimensionality of the nested hierarchy. Firstly, we show how one can increase the dimensions of a linear time-keeper by likening our topology to the face of a clock (A), where completion of the circling hand of a faster dimension (i.e. dashed arrow) moves a slower dimension forward by one tick (i.e. solid arrow). In the example shown there are 8 nodes per dimension, such that the number of unique time points each dimension can represent increases in a piecewise linear fashion (B) that is proportional to the number of nodes in prior dimensions (i.e., 8 unique time points for 1 dimension [D_1] of 8 unique nodes; 64 unique time points for 2 dimensions [D_2] of 16 unique nodes; 512 unique time points for 3 dimensions [D_3] of 24 unique nodes). We continue the trajectories of each dimension's informational capacity to show the improvements that additional dimensions have on storage cost. We show both the typical (C-D) topology of a synfire chain from other modelling works (Diesmann et al., 1999; Itskov et al., 2011) as well as the novel hierarchical (E) topology described here. In the initial description of synfire chains (Diesmann et al., 1999), it was only necessary for a single dimension to pass activation through consecutive groups of excitatory (E, blue, nodes) cells (C). The addition of inhibitory (I; red nodes) cells in a "Mexican-hat" topology allowed for the emergence of winner-take-all behaviour (D), which allows temporal context to emerge in a broadly tuned population (Itskov et al., 2011). The hierarchical topology (E) adds further complexity by doubling-up on the winner-take-all framework. This scalable and compact assembly allows an additional inhibitory node (off-node, or O cell) to terminate persistent activation in an excitatory population (E node) when it receives a signal from an additional excitatory node (propagation-node, or P cell). Simultaneously, this propagation-node feeds into consecutive E nodes, permitting signal transmission once lateral inhibition subsides from terminated predecessors. The P cell also initiates feed-forward excitation in the first E node of any existing higher dimensional chains (D_{+1}), as well as feed-back termination of any existing lower dimensions (D_{-1}). This enables the simultaneous and persistent activation of multiple temporal dimensions, akin to a ticking clock (Barnard, 2002; Friston, 2018). A dynamic visualisation of this process can be found in the video file of [Supplementary Fig. 4](#).

which operates by discretising input to avoid repetition induced conjunction errors. Here, a sparsely encoded unique index binds cortical content to a moment in time (see Fig. 1B). Similar to other models (Bowman and Wyble, 2007), this binding process can trigger an attentional-blink phenomenon, where indices occurring very close together in time are poorly encoded. In exploring the functionality of this phenomenon, we find that these binding induced attentional deficits function to further increase episodic distinctiveness, creating boundaries between encoded events. Altogether, the current modelling work explores a plausible framework to generate the temporal signatures observed in human EEG/MEG signals, and what functional role these observed physiological signals might play in information processing and episodic memory formation.

Our model comprises three distinct mechanisms (as shown in Fig. 1) which independently implement timing, binding, and information content, and together encode episodic memories that can be dynamically detected via cortical temporal signatures (Michelmann et al., 2016). In

doing so, we aim to provide theoretical evidence for the inhibition-timing (Klimesch et al., 2007) and information via desynchronisation hypotheses (Hanslmayr et al., 2012). As such, information representation occurs in a neocortical (NC) area (Fig. 1A), where an alpha desynchronisation indicates information processing (Hanslmayr et al., 2012), as described in previous modelling work (Parish et al., 2018). In the current work, we create an intrinsic and dynamic alpha frequency through recurrent excitatory-inhibitory interactions (Fig. 1A, left-hand section; blue excitatory node & red inhibitory node), where the frequency is dependent on the length of inhibitory post-synaptic potentials (Brunel, 2000). This allows changes in the environment to cause phase reset patterns with some specific temporal pattern (Fig. 1A, right-hand section; phase angle time series punctuated by event-driven phase-resets), thus conveying temporal information (Canavier, 2015; Ng et al., 2013; Schyns et al., 2011). This mechanism allows us to explore how phase-resets (and therefore information) might be generated relative to a gate-keeping alpha frequency (Klimesch et al., 2007),

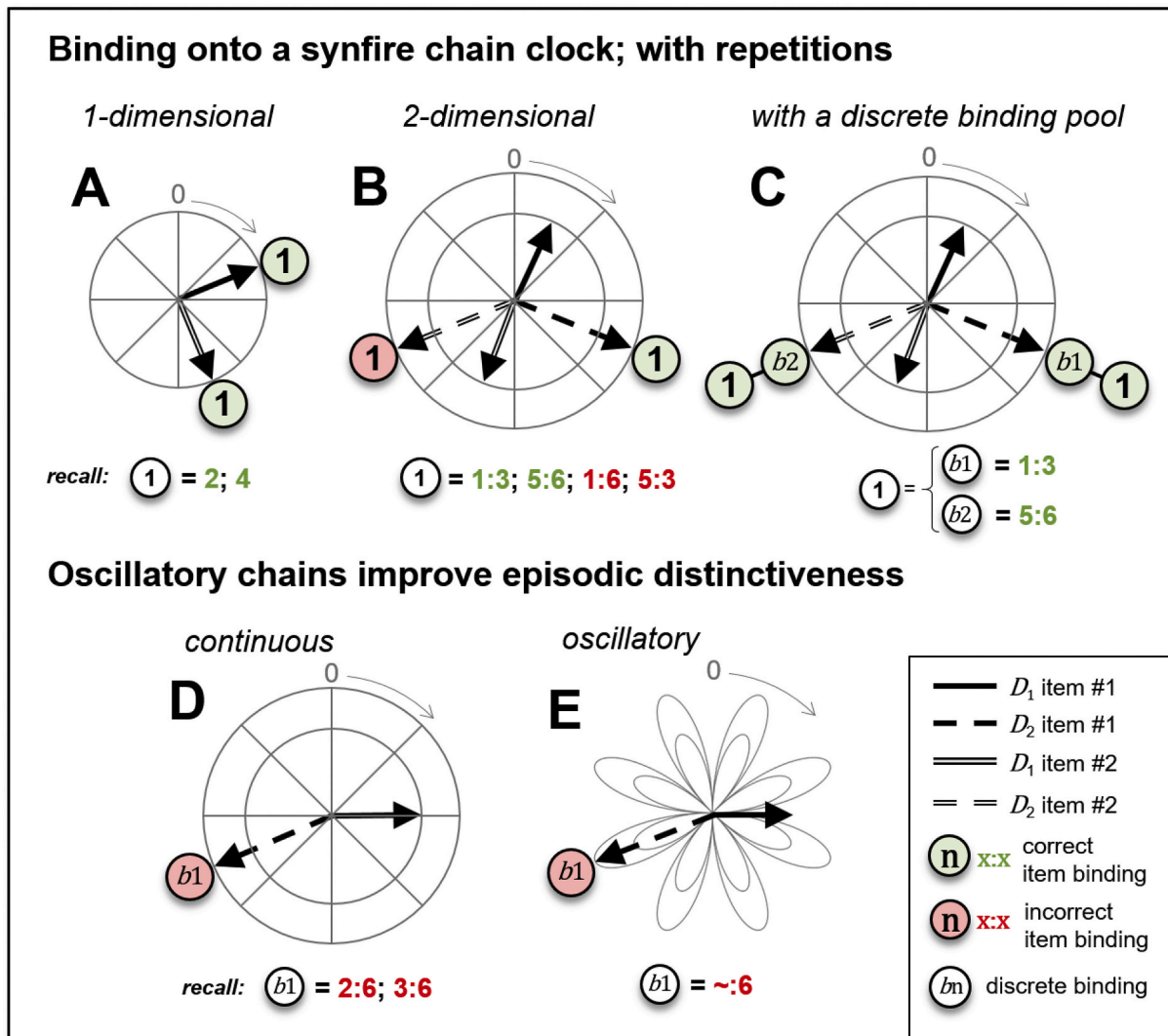


Fig. 3. Consequences of binding content onto hierarchical synfire chains that are used to represent temporal positions. In A-C, we show that if one increases the dimensionality of the synfire chain, then one can no longer directly bind content repetitions without the use of a discretising binding pool. If the synfire chain is 1-dimensional (A), then each repetition of content is bound to a unique temporal position, ensuring that later reactivation of content is unambiguous. As one considers 2-dimensional chains (B), however, then each repetition of content is incorrectly bound to multiple temporal positions, due to the recurrence of faster chains for every tick of a slower chain. This necessitates the instantiation of a binding pool (C), which discretises content into unique binding contexts akin to other models (Bowman and Wyble, 2007), allowing the recovery of the original content upon reactivation. In D-E, we show another complication in the use of hierarchical synfire chains for the representation of time. When content occurs on the border between nodes (D), then it is again ambiguously bound to multiple temporal positions. This issue can be addressed with the introduction of oscillatory synfire chains (E), which have down-phases during which time content cannot be fully bound. This oscillatory mechanism increases episodic distinctiveness (i.e. segregation into distinct temporal episodes), at the cost of reduced content specificity.

by adjusting the timing and strength of events relative to the intrinsically oscillating phase of this cortical representation (shown later in Fig. 4). A time-series of the local field potential (LFP) is calculated as the summation of spike events, filtered by a band-pass filter within a particular range (see Appendix 1.1). A Gaborfilter is then applied, where the absolute or the angle of the resultant complex numbers is taken to approximate power or phase, respectively.

During encoding (Fig. 1; blue top-down arrows), event-triggered activation is forwarded to the binding pool area. This discretises events consistent with the idea that the brain allocates unique tokens (Bowman and Wyble, 2007), allowing us to differentiate between repeating stimuli in a sequence. Here, the occurrence of a stimulus is treated as a distinct event through the activation of a selective population of units in a winner-take-all environment (Fig. 1B, left-hand section), implemented as long-range inhibitory and short-range excitatory connections (commonly termed a “Mexican-hat” topology”). In order to prevent runaway excitation in this event-driven and broadly tuned population, an additional inhibitory group was required. This received slow ramping excitatory input, eventually clamping down on the whole excitatory population. As such, we define this additional inhibitory group as “off-switch” cells. This mechanism has the additional effect of causing an attentional deficit immediately after a successful binding (shown later in Fig. 6), which we found to increase the episodic distinctiveness of encoded memories by creating clear boundaries between events. During the binding process, a group of unique binding pool units are associated to any active cortical unit via a calcium dependent learning rule (Graupner and Brunel, 2012). As their local weights decrease during this process, which effectively models a form of hetero-synaptic long-term-depression (Volgushev et al., 2016), active binding groups become less likely to compete during successive events. Thus, active bindings are unique to the bound event. Concurrently, active temporal units (Fig. 1C, described in Figs. 2 and 3) are also associated with binding pool units, thus sequencing the timing of events as they occur. Once the hierarchical time-keepers are re-started in a cued-recall paradigm, the relevant binding pool units become active at specific moments in time (Fig. 1; green bottom-up arrows), causing a temporal pattern of events to be re-instantiated in the neo-cortex. As the timing mechanism is oscillatory, this allows us to explore the functionality of oscillations in providing temporal reference frames in a more general sense (shown later in Fig. 7).

In exploring the use of a feedforward neural substrate for the encoding of time (see Fig. 2), similar to other models (Itskov et al., 2011; Rolls and Mills, 2019), it was found that oscillations increased the quality of memory encoding by creating clear boundaries between temporal reference frames (see Fig. 3). This motivates us to further explore how hierarchical oscillators might regulate temporal perception (Barczak et al., 2019; Lakatos et al., 2005; Tai et al., 2020), examining the benefits and pitfalls of an oscillator-based model for serial order (see Fig. 3), similar to other models (Brown et al., 2000). Feedforward chains, often called synfire chains, are consecutively connected cell assemblies (see Fig. 2C and D) that have been theorised to enable feed-forward signal transmission across the brain (Diesmann et al., 1999). Feed-forward synfire activation is thought to be the best enabler of fast communication with high temporal precision. This is believed to be necessary for the distributed time-keeping that occurs during sensory and motor events (Mauk and Buonomano, 2004), possibly by enabling target cells to conjunctively represent distinct elements of a stimulus (Fries, 2005). Models of such synfire chains have shown that this kind of signal transmission can operate within a noisy environment (Diesmann et al., 1999), can co-exist within a randomly connected embedding network (Kumar et al., 2008), and might even naturally emerge in a plastic and locally connected environment (Fiete et al., 2010). It can be further demonstrated that a feed-forward synfire architecture can support temporal encoding (Itskov et al., 2011), predicting that temporal sequences can be internally generated, being reliable from trial to trial, context dependent and long lasting, in a manner similar to time cells

(Eichenbaum, 2014). However, a common criticism of such a means to model time is that the length of the chain must increase linearly with the desired duration (Shankar and Howard, 2012), especially important considering that humans can integrate experiences in time and space within the realm of milliseconds to minutes (Mauk and Buonomano, 2004).

Considering this, a goal of the current modelling work is to thus reduce the physical requirements of synfire chains in the encoding of longer temporal durations, which might be of interest from a systems as well as a physiological perspective. We achieve this by instantiating a hierarchical feed-forward chain (see Fig. 2), echoing principles of a recently published model (Rolls and Mills, 2019), where sequential cell assemblies maintain persistent activation in a feed-forward manner (Goldman, 2009; Itskov et al., 2011). To do this, we envisage a simple cell assembly of Hodgkin-Huxley neurons (Hodgkin and Huxley, 1952) that can be scaled up to encode for multiple, simultaneous and interacting temporal hierarchies. This cellular assembly exists as a compact unit with specific feedforward and feedback connections (see Fig. 2E), initiating and terminating persistent activation upon the completion of hierarchical sequences. We thus instantiate a hierarchy of synfire chains, where completion of a higher-dimensional faster sequence initiates the transmission of persistent activity to the next node in a lower-dimensional slower sequence. As such, higher-dimensional sequences repeat at every node of the lower-dimensional sequence, decreasing the physical requirements of feedforward chains in the encoding of long temporal durations (see Fig. 2B). A moment in time is then marked as the concurrent activation of multiple temporal positions on simultaneous hierarchies, much like the multi-dimensional hands of a ticking clock (see Fig. 2A).

However, there are associated costs with our hierarchical implementation, namely, repetitions and conjunction errors (see Fig. 3). Repetitions occur when the same content is shown multiple times, where there is a marked difference if one were to bind repeating content directly onto a 1-dimensional (Fig. 3A) or a multi-dimensional (Fig. 3B) time-keeping device. There is no opportunity for confounds in the former, as each sequential synfire node represents a unique temporal position. In the latter, faster-dimensional chains repeat for every node of a slower-dimensional chain, meaning that temporal positions are represented by unique combinations of hierarchical nodes. This means that confounds are incurred at recall when a repetition of content is directly bound onto multiple hierarchical nodes, as the encoded content will get reactivated at any combination of those respective nodes. This problem is overcome when one discretises content through the use of a broadly tuned binding pool. Here, each repeating item is treated as a wholly new event, meaning it will be uniquely transcribed onto any given multi-dimensional temporal position (see Fig. 3C). Whilst the necessary addition of a binding pool increases storage cost, we expect this to be a fixed size population of broadly tuned units, providing a highly distributed representation (O'Reilly and Munakata, 2000) that overall, does not impose too much on storage constraints when representing longer temporal durations.

The secondary cost associated with the adoption of a hierarchical representation of time, regardless of substrate, is that of conjunction errors (Botella et al., 1992; Chennu et al., 2011). The conjunction errors we are interested in are the erroneous binding of content to multiple neighbouring moments in time. These can arise when content occurs at the boundary of temporal windows, especially those at slower-dimensions, as content is then incorrectly bound to multiple temporal positions in the hierarchy at once (see Fig. 3D). Interestingly, an effective solution to these conjunction errors is to switch from a continuous representation of time to an oscillatory one, as has been shown to be useful for auditory (Tai et al., 2020) and visual (Barczak et al., 2019) perception. This was achieved in the model by incorporating ramping-up periods in our synfire-chain assemblies, similar to those observed in the hierarchical ramping cells of the lateral entorhinal cortex (Tsao et al., 2018), that slow down transmission from one node to

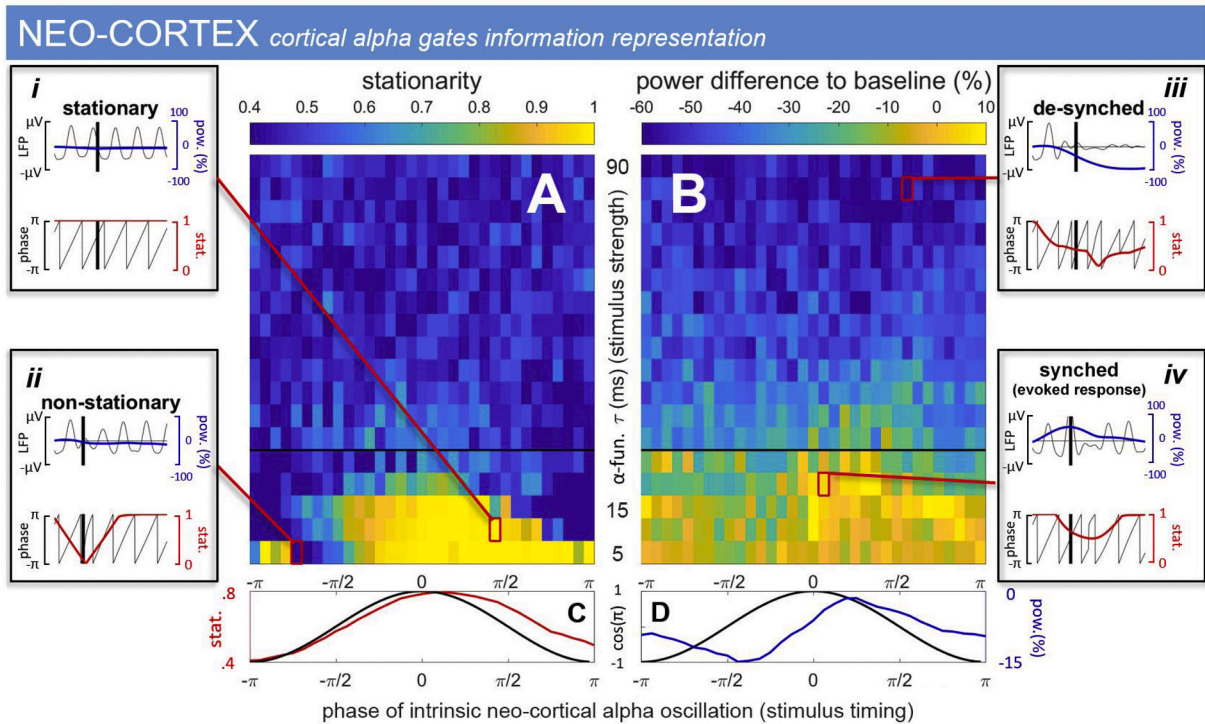


Fig. 4. Effect of input stimulus strength & input timing on the modelled alpha rhythm.

Evaluating the parameter space for a stimulation of a given length to cause a desynchronisation and phase-reset of the intrinsic cortical oscillation. Large inputs desynchronise and reset the phase of the intrinsic rhythm, however small inputs only do so dependent on the current phase of the gating rhythm. A cortical stimulation is simulated as a Poisson distributed spike-train of a given number of spikes, multiplied by an Alpha-function ($F[\alpha]$) described in Equation (12) in the methods section (see supplementary section). Here, we simulate many thousands of trials whilst varying the time constant (τ), which modulates the length of that function. In panels A & B, we plot the stationarity (A) and power difference to a baseline period (B; the mean of a period of 500 ms, ending 250 ms prior to stimulus onset) of the simulated cortical population, with respect to the τ of the α -function (y-axis) and the cosine phase at the time of stimulation (x-axis), allowing us to examine the strength and timing of the stimulus and its effect on a simulated cortical population. In A, stationarity is calculated as the similarity (RSA) of the stimulated period in relation to a pre-stimulus period, where any value below 1 indicates the existence of phase-resets. When we collapse vertically (C; where $\tau \leq \sim 25$ ms, indicated by the black horizontal line in A), the relationship between the intrinsic phase and time of stimulation is fully expressed, where the cosine wave of the intrinsic oscillation (C; black line) closely matches the stationarity of the population after stimulation (C; red line). We similarly consider power differences to a baseline period (B), where a positive or negative value indicates a synchronisation or desynchronisation of the intrinsically generated oscillation, respectively. Collapsing vertically, i.e., over stimulus strength, (D; where $\tau \leq \sim 25$ ms, indicated by the black horizontal line in B), one can also see how power desynchronisation tracks the intrinsic cortical phase at presentation, albeit with a small lag. Panels *i-iv* show individual trials, where red lines and boxes tie to the corresponding τ and phase on the y-axis and x-axis, respectively. A vertical black line indicates the time of the peak of the α -function, i.e. the τ . On the left-hand axes, the local field potential (LFP) is shown above the intrinsic phase over time, with power deflections and stationarity similarly shown on the right-hand axes in blue and red, respectively. We highlight examples of trials where the intrinsic phase during stimulation is stationary (*i*) or non-stationary (*ii*), as well as when oscillatory power is de-synchronised (*iii*; “de-synched”) or a transient evoked response occurs due to synchronisation of input and phase (*iv*; “synched evoked response”).

another in the inter-dimensional hierarchy. By implementing this oscillatory segregation in our nested chains, we were able to improve the episodic distinctiveness of temporal encoding within the model, albeit with the loss of any content that occurs within oscillatory troughs (see Fig. 3E). This is akin to the phenomenon of the attentional blink – described as a loss in temporal perception occurs for stimuli very close together in time. This suggests that the role that oscillations might play, is segregating temporal episodes into discernible chunks, as a previous model has also suggested (Brown et al., 2000).

3. Results

3.1. Cortical alpha as a mode for information representation

We conduct several simulations using our model to evaluate its three distinct components (see Fig. 1). Firstly, we consider how information is generated relative to cortical alpha phase, given a stimulation of a given length (Fig. 4). This allows us to examine the inhibitory gating effect of cortical alpha oscillations, where the timing of an event is just as important as its strength when deregulating activation and representing information (Canavier, 2015; Ng et al., 2013; Schyns et al., 2011). This

also informs the parameters used to simulate the representation of a stimulus for later simulations, allowing a stream of events to be consistently encoded.

In evaluating the effect of a stimulus on the stability of our intrinsically generated oscillations, we explored both the length of the stimulus, (i.e. the time constant, τ , of the $F[\alpha]$ described in Equation (12) of the methods section) and the phase of the intrinsic cortical frequency at which it was presented (Fig. 4; $-\pi \rightarrow \pi$). Here, we see how a small stimulation causes no phase-reset if it is presented near the peak of the intrinsic oscillation (Fig. 4A; $\tau \leq \sim 20$ ms), i.e. when the population has recently fired and is currently being inhibited by local circuitry. As the stimulation increases in length, it causes phase-resets no matter at which phase it was presented. Interestingly, if even a small stimulation occurs in the trough of the intrinsic oscillation, i.e. when the population is less inhibited and gradually self-exciting, then there is a high likelihood of causing premature activation in the network and inducing a phase-reset. Similarly, for small stimuli there is a power synchronisation of the intrinsic oscillation if they are presented near the peak of the intrinsic frequency (Fig. 4B; $\tau \leq \sim 20$ ms), where they cause an additive evoked response. This bears much resemblance to our previous modelling work (Parish et al., 2018), where weak, temporally non-specific activation

was found to similarly synchronise cortical alpha oscillations by increasing the firing rate of neurons at the peak, but not the trough, of a given frequency. The additional exploration here finds that the timing of that stimulation is important, where a desynchronisation is caused even by small stimulation if it occurs just before the peak of the intrinsic frequency (Fig. 4D). This indicates an increase in information, as stimuli of interest shift in phase relative to the synchronised and uniform alpha oscillations over the rest of the brain (Hanslmayr et al., 2012; Klimesch et al., 2007).

3.2. Encoding & reactivation of an episodic sequence

We next go on to simulate a single trial of our model (Fig. 5), where the relative temporal relations within a sequence of cortical events is discretely encoded and reactivated. Here, we use RSA to detect the re-instatement of an encoded sequence at recall. This allows us to explore how information is represented in the cortex through desynchronising the intrinsic rhythm (Hanslmayr et al., 2012), conveying a temporal phase-reset signature that can be dynamically decoded upon reactivation (Michelmann et al., 2016).

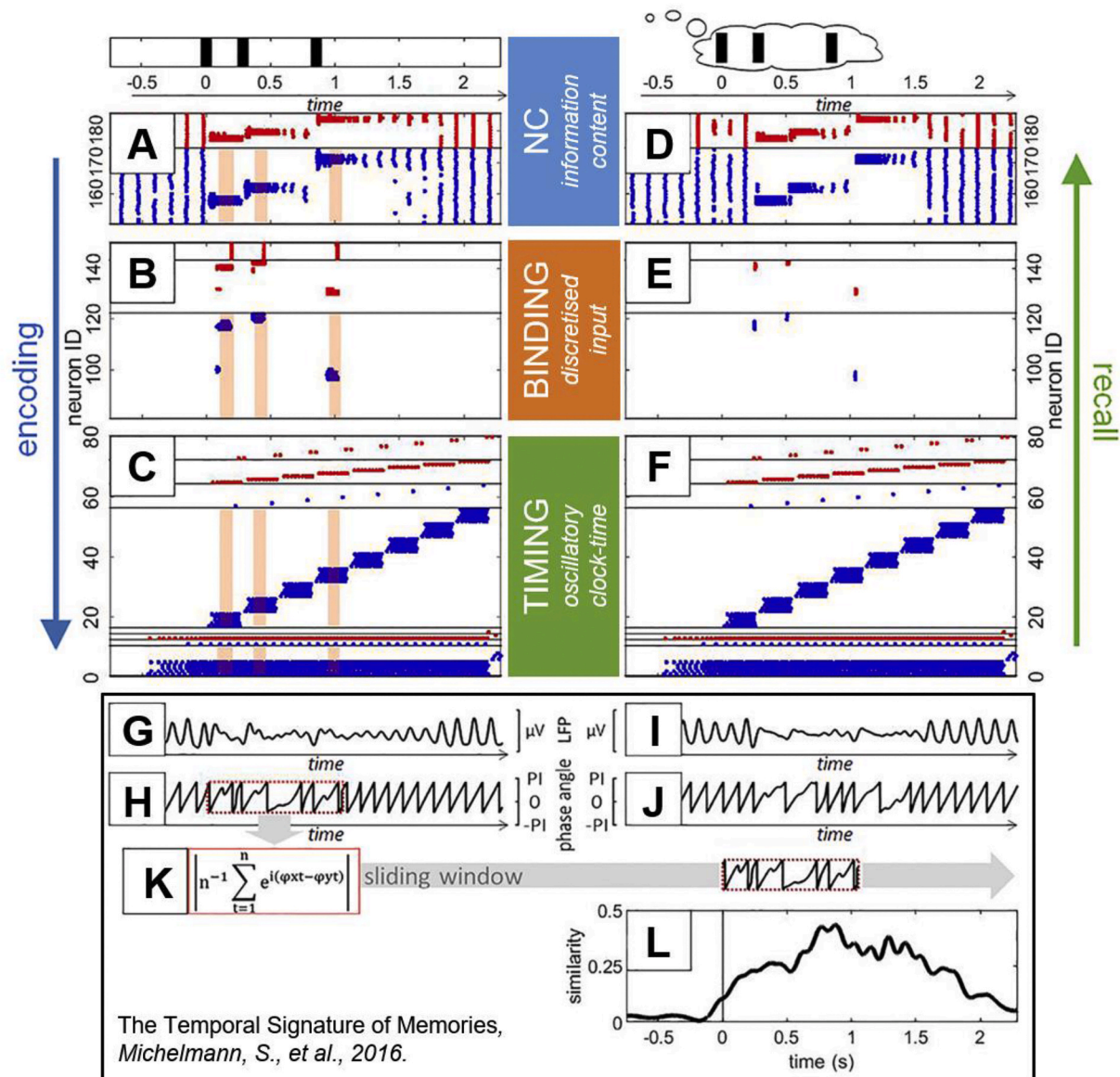


Fig. 5. Encoding & replaying a single sequence.

Raster plot of a single simulation (A-F; blue/red dots = excitatory/inhibitory spike events) and subsequent phase-angle RSA (G & I: local field potential (LFP); H & J: phase-angles; K: RSA method and application; L: similarity signal through time), for encoding (A-C; left panels) and recall (D-F; right panels). At encoding, a sequence of events (top left panel; black lines) were fed into a random selection of cortical excitatory units (A), which became active at the expense of the population due to a “Mexican-hat” topology. This triggered activation in a unique group of selective binding pool units (B), which was itself terminated by an additional “off-switch” node to prevent run-away excitation (red spike events, top line-separated panel). During this time, hierarchical synfire chains maintained temporal rhythm through sequential activation of cellular assemblies (C). Long-term-potential (LTP) worked to bind any active units together in time, from the temporal region to the binding pool region, and from the binding pool region to the cortical region. Long-term depression (LTD) worked to reduce the weights of active binding assemblies, ensuring a sparse coding for each incoming cortical stimulus. Orange shaded regions are applied to the raster plots at encoding (A-C) to visualise periods of synaptic modification, where calcium amplitudes were above the threshold for potentiation. During recall (D-F; right panels), the re-started temporal region reactivates relevant bound events in the correct temporal order. The disruption of the intrinsic cortical oscillation can be seen in the LFP (G & I), where a diminution signals a desynchronisation in the dominant frequency (set to ~8Hz in this simulation). A subsequent phase-reset pattern at encoding is highlighted in the red dotted box (H), which was used in an RSA approach (K) to detect the re-instatement of a similar phase-reset pattern at retrieval (L).

In Fig. 5, neo-cortical (NC) assemblies were designed such that they intrinsically oscillated at a particular frequency, determined by parameters for excitation/inhibition interactions (Brunel, 2000). In addition, a winner-take-all environment was instantiated, as has been theorised in models of visual working memory (Itti et al., 1998). Hypothetically, this ensures that only one locally connected neuronal group can be active at any one time, minimising the simultaneous activation of multiple representations in a distributed manner. As can be seen in Fig. 5A, parameters were chosen to enable activation to spread through the entire excitatory population before inhibitory interactions had time to clamp down, thus allowing intrinsic oscillations to emerge. Once input was fed into a group of excitatory units (Fig. 5A; sustained excitatory spike events, depicted as blue dots), the selective topology can be seen inhibiting competing representations (Fig. 5A; sustained inhibitory spike events, depicted as red dots). This subsequently causes a desynchronisation in the ongoing alpha oscillation (Fig. 5G; local field potential), a phenomenon shown in many studies (Haegens et al., 2011; Hanslmayr et al., 2011a; Griffiths et al., 2019) to be related to neuronal activation. During this desynchronised period, the phase-angle time-series shows evidence of phase-resets (Fig. 5H; red-dotted box), as the on-going intrinsic oscillation is externally affected through its representation of incoming stimuli. This indicates that these phase-reset periods are linked to periods of event-related cortical activation, lending theoretical evidence to the argument that phase-angle time-series can be used to decode information content (Canavier, 2015; Ng et al., 2013; Schyns et al., 2011).

The binding pool within the model was developed with similar intentions as other models (Bowman and Wyble, 2007), where a unique node was selected from a broadly tuned population to encode an event. We argued earlier that this method allows for repetitions (Fig. 3), where each presentation of a stimulus is treated as an independent event. In this way, a binding node is only required to activate during an event-related cortical activation, as can be seen in the raster plot of Fig. 5B. Here, parameters were chosen such that intrinsic oscillatory activity is not sufficient to cause activation in the binding pool. This is fulfilled by a relatively large synaptic time constant to gate cortical-binding projections, requiring sustained input to trigger binding activity. It was also important to obtain weight variation on these projections by sampling from a normal distribution, to increase the likelihood of winner-take-all behaviour during event-related sustained input. As depicted in Fig. 1B, a global “off-switch” inhibitory cell (red node marked O) adds an additional safeguard mechanism to prevent runaway activation across the excitatory population, operating to inhibit the entire binding pool once sustained excitatory input reaches a threshold. Active binding pool units engage in learning, making bindings between the active cortical content layer and the currently active temporal units which together index a moment in time (indicated by orange shaded regions in Fig. 5A–C). During this time, the connections between active binding pool assemblies undergo long-term-depression, meaning that these bound units would not be able to compete upon successive activations of the binding pool due to its highly selective topology. This ensured that each binding pool assembly uniquely indexed an event in time.

Fig. 5C also shows a raster plot of our hierarchical, clock-like synfire chains. Once these chains are re-started with an initiating burst in Fig. 5F, the relevant binding and cortical clusters are then successively activated dependent on the combined activation of synfire hierarchies (Fig. 5D and E). We then examine our model in light of recent experimental findings (Michelmann et al., 2016), where unique temporal signatures were detected for dynamic stimuli in the phase-angle time series. As such, we show the phase-angle time series of cortical regions at encoding (Fig. 5H, at 8Hz), where a phase-reset pattern coincides with the presentation of the pattern (red dotted box). Using RSA, we can then compare this phase-reset pattern at encoding with the phase-angle time series at recall (Fig. 5J), resulting in a similarity time-series that peaks at the time of the re-instatement of the encoded pattern in cortical regions

(Figure 5L).

As shown in Fig. 5F, the recall phase entailed restarting the hierarchical synfire chain, reactivating any relevant bindings in sequence. During this time, a pronounced alpha desynchronisation is also observable (see the LFP in Fig. 5J), building upon previous modelling work (Parish et al., 2018) that indicates that this can predict both successful memory encoding and recall (Fell and Axmacher, 2011; Hanslmayr and Staudigl, 2014; Khader et al., 2010; Klimesch et al., 2005; Waldhauser et al., 2016). A notable lag in cortical reinstatement (Fig. 5D) indicates that the upwards direction of retrieval processes takes longer than the downwards direction of encoding processes, which is also indicated by experimental findings (Michelmann et al., 2016; Griffiths et al., 2019). Neurophysiologically, there are likely to be many neuronal layers for detecting and processing stimuli that would subsequently increase this recollection lag. In the model, however, this is mostly since binding units fire late in their respective temporal window (as indicated by Fig. 5E). This lag could be reduced within the model by increasing upwards directional weights to encourage binding units to activate earlier in their window. However, this could have the undesirable effect of shifting activation forwards from encoding to recall, as events that are bound at a later point during the relatively broad window of our self-completing chain (~200 ms in length, ~5Hz), might be reactivated at an earlier point. In response to this, one could reduce the error by choosing a finer temporal dimension for the fastest, self-completing synfire chain. Bindings should then be encoded and recalled with more temporal precision. Such a notion might go some way to addressing why high-frequency gamma oscillations (>40Hz) are prevalent during episodic memory formation (Sederberg et al., 2007). This line of reasoning has also been noted by Fell and Axmacher (2011) and other models of sequence encoding (Jensen et al., 1996), who argue that gamma provides a fine-grained window of activation to maximise precise communication and learning (Fries, 2015).

3.3. The binding pool enhances the episodic distinctiveness of memories

Next we explore the relationship between the timing of two target stimuli and weight change in the model (Fig. 6). This analysis examines the attentional-blink phenomenon, as in other models (Bowman and Wyble, 2007), which is produced here as a by-product of an inhibitory off-node, the primary purpose of which is to control over-excitation in a broadly tuned population. By encoding events very close together in time, we examine the limitations of binding more generally, where an attentional-deficit might actually enhance episodic distinctiveness by clearly separating the boundaries between encoded events (Wyble et al., 2009). The “binding” element of our model (Fig. 6) entails that events are discretely encoded as novel indexes using a binding pool of a fixed capacity. We can evaluate the limitations of this binding process by seeing what happens when two target stimuli are presented when varying temporal lags between them. Over many simulations, we can determine that the closer these two target stimuli (T1 & T2) are presented in time, the more likely they are indexed by a single binding, reducing the episodic distinctiveness of these separate events and potentially increasing conjunction errors upon reactivation. This can be seen in Fig. 6, where for lags of ≤ 150 ms, we see that the binding pool capacity of the model is only decreased by the amount of one binding (Fig. 6A and B; grey shaded, ~15% binding pool capacity per binding). During this time, we can show that the T1 binding is often outcompeted by the subsequent T2 rival. Here, weight change is near maximal for the encoding of the T2 stimulus (Fig. 6B; all lines, ≤ 150 ms), whilst a decrease in T1 weight change occurs if it is followed by a T2 (Fig. 6A; black solid line, ≤ 150 ms). This is likely due to the “Mexican-hat” topology of our cortical network, which promotes the activation of only one representation at a time. We verify this theory by assessing the consequences of the content not changing between target stimuli, i.e. if the T1 is repeated (Fig. 6A; black dashed line). As can be seen, in this case there is no reduction in T1 efficacy.

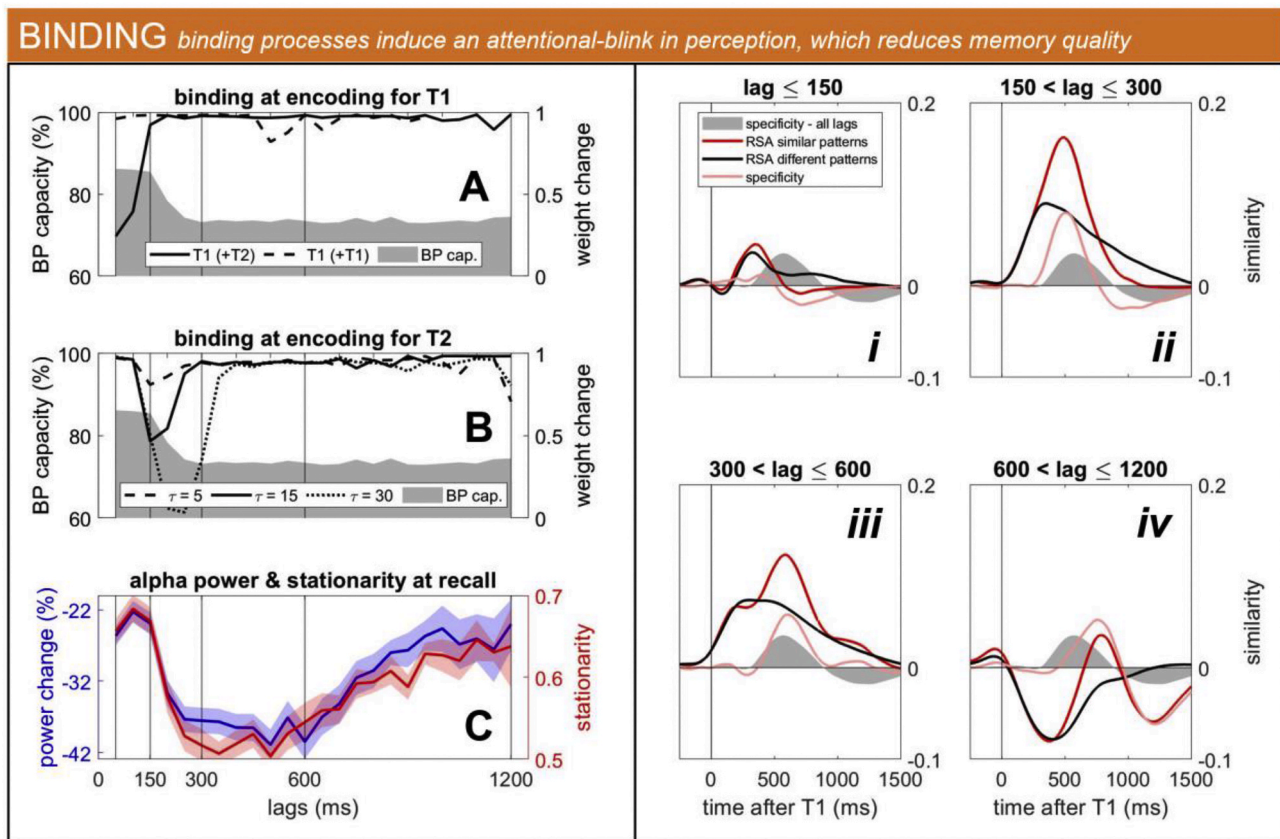


Fig. 6. Evaluating the attentional blink & episodic distinctiveness.

Presenting two target stimuli (T1 & T2) to the model, where the T1 occurs before the T2. We simulate 2000 trials, each with a random time for the T1 & T2, thus varying the temporal lag between them. In the left-hand panels, we show the lag between the T1 & T2 on the x-axis with 50 ms bin width. In panels A–B, we show weight change of any active binding pool neurons at encoding on the right-hand axis, where a value of 1 indicates a strong replication of the successful indexing of neo-cortical content across trials. Similarly, on the left-hand axis, we show the remaining capacity of the binding pool (BP) after encoding, i.e. the proportion of weights that have not been reduced by LTD and thus are still capable of indexing further events. This allows us to see how many bindings are made at any given lag, where $\sim 15\%$ capacity is used per binding. In panel A, we show the accuracy for the T1 stimulus, both when a T2 (black line) or a repeating T1 (dashed line) stimulus occurred afterwards. As a random neo-cortical subpopulation is activated for each target stimulus, a repeated T1 is discerned as the same cortical population being activated twice in succession. In panel B, we show the accuracy for the T2 stimulus, this time varying the strength of inhibition that the binding pool “off-node” exerts on the population ($O \rightarrow E \tau_S$). We show the default parameter ($\tau_S = 15$ ms; black line, 2000 trials), as well as a lower value ($\tau_S = 5$ ms; black dashed line, 2000 trials) and a higher value ($\tau_S = 30$ ms; black dotted line, 2000 trials). This analysis allows us to explore the parameter that causes an “attentional-blink” phenomenon in this model, where the T2 stimulus has lower accuracy if the lag between T1 and T2 is small. In panel C, we show power change (blue line) and phase similarity (red line) relative to a baseline period (the mean of a period of 500 ms, ending 250 ms prior to stimulus onset) of the total neo-cortical population, i.e. independent of which target stimulus is active, at recall (shaded regions indicate 95% confidence intervals). In the right-hand panels (i–iv), we show the mean similarity (RSA) of the phase of each trial at recall to that of similar patterns (i.e., where T1 & T2 lag is similar; red lines), to that of different patterns (i.e., where T1 & T2 lag is dissimilar; black lines), and the content specificity (i.e., similarity to same minus to different patterns; pink lines). The overall content specificity of all trials is shown in the grey shaded area on each of i–iv, though we separate data by lag for each panel. This allows us to see how much the specificity for each lag region (pink lines) contributes to the overall specificity (grey shaded area). We here determine lag regions by looking at the left-hand panels, where vertical black lines have been drawn to mark the boundaries of behaviourally distinguishable regions. The underlying components of similarity to same (red) and similarity to different (black) patterns further allows us to examine why the overall content specificity varies by lag region, informing our discussion as to what we might consider interpretable signal using this method.

When we increase the temporal lag between the two target stimuli, episodic distinctiveness increases as one begins to make multiple bindings for multiple target stimuli, though a lapse in binding capability at this junction begins to occur, in what is known as the “attentional-blink” phenomenon. Between a lag of 150 & 300 ms, there is a drastic reduction in the weight efficacy of the encoding of the T2 stimulus (Fig. 6B; all lines, $150 < \text{lag} \leq 300$ ms), whilst that for T1 remains very high (Fig. 6A; both lines, $150 < \text{lag} \leq 300$ ms). This is due to the “off-switch” node of our binding pool population, whose main priority was to stop runaway excitation from occurring after a successful binding. However, when the binding pool is inhibited, it is impaired in its capacity to register the next incoming stimulus. We explore several parameter settings for the synaptic time constant (τ_S) of the binding pool “off-node” to the excitatory population, whereupon we clearly see how a larger value (i.e. larger inhibition) leads to a further reduction in T2 efficacy at short lags

(Fig. 6B; black dashed line $\tau = 5$, black solid line $\tau = 15$, black dotted line $\tau = 30$). This interesting finding indicates the secondary role that such an “off-switch” might have evolved to play in improving the quality of our episodic memories, by segregating episodes into clearly distinguishable bindings, despite the loss of attention for very short lags.

As the lag increases past 150 ms, binding pool capacity is further reduced (Fig. 6A and B; grey shaded region), indicating that another indexing has taken place (upon which intra-binding pool weights are reduced by activation induced LTD). When it is clear that the majority of simulations have made two distinct bindings (Fig. 6A and B; grey shaded region, $\text{lag} > 300$ ms), we see that both T1 and T2 efficacy are high (Fig. 6A and B; weight change $> \sim 0.8$), indicating that both target stimuli have been successfully encoded as distinct episodes.

In addition to the binding mechanics at encoding, we also explore the stationarity and power deflections of the cortical population at recall

(Fig. 6C; stationarity in red, power change from a baseline period in blue). This was done to assess the quality of the binding process upon reactivation in the non-specific manner available to most EEG/MEG studies, where stationarity and power track the imaginary and real components of a Fourier transformed complex time-series. In doing so, we show how asynchronous firing can cause desynchronisations in two different ways, namely, by suppressing power through irregular spike patterns and by resetting the intrinsic phase (explored in Fig. 4). Initially (<150 ms), the stationarity and synchronisation of the cortical population at recall closely matches the binding pool capacity (Fig. 6A and B; grey shaded), indicating the singular binding made at encoding was recalled as a single item (Fig. 6C; ~20% desynchronisation & ~0.3 reduction in stationarity per represented item in the phasic signal). Between lags 150–300 ms, there are variably 1–2 items successfully

encoded and recalled, indicated by reducing values in cortical synchronicity and stationarity. However, as we are considering a window centred over the midpoint between the target stimuli, we see a gradual increase in the length of oscillatory stability between the T1 and T2 for increasing lags. This has an important effect on the quality of the phasic temporal signatures that are later used to detect the re-instatement of content.

In Fig. 6i–iv, we show how one can use the RSA approach to detect the re-instatement of unique temporal signatures that were identified at an encoding stage, as described by Michelmann et al., 2016. Using this method, one can calculate the mean of RSA to all similar patterns (Fig. 6i–iv; red lines), as well as the mean of RSA to all different patterns (Fig. 6i–iv; black lines). The difference between these is termed the specificity of the similarity measure (Fig. 6i–iv; pink lines), i.e. how

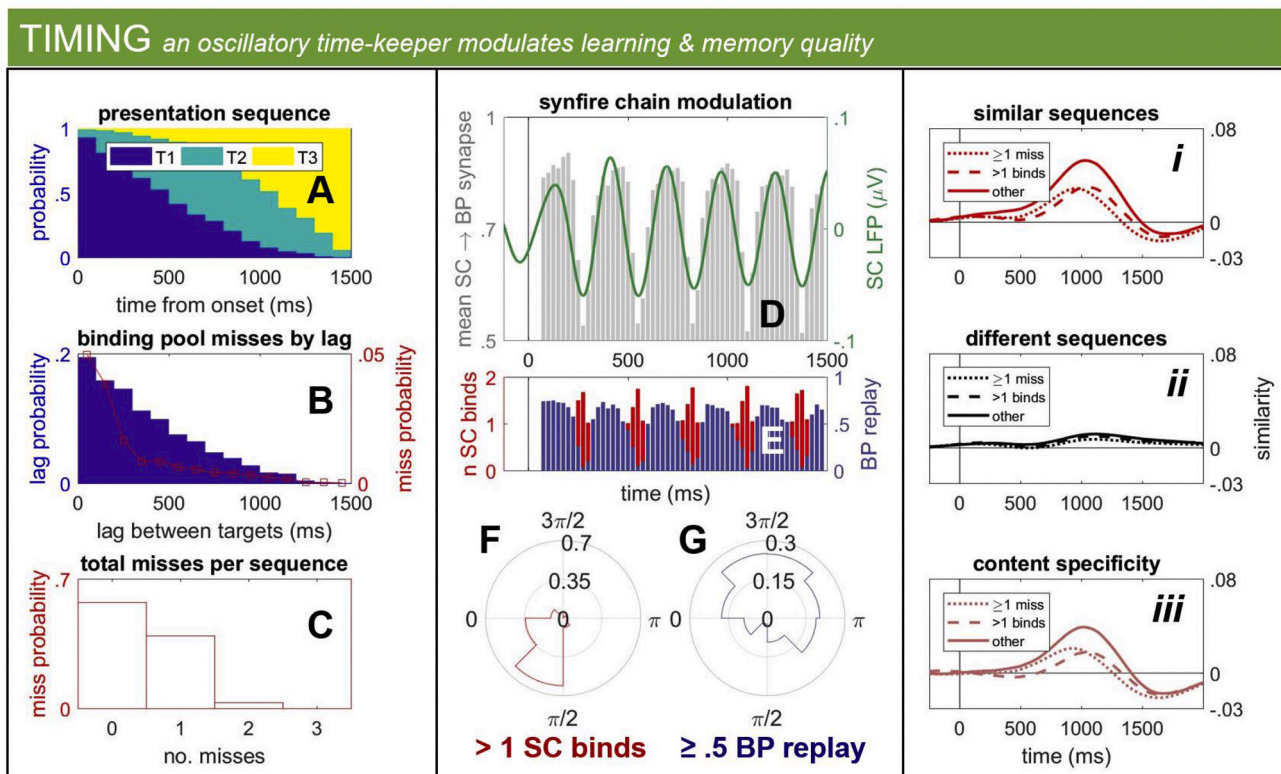


Fig. 7. An oscillatory segregation of time.

Presenting three target stimuli (T1, T2 & T3) to the model, where T1 occurs before T2, and T2 occurs before T3. We simulate 2000 trials, each with a random time for T1, T2 & T3, thus varying the temporal lags between them. The distribution of target stimuli over a 1500 ms period is shown as a stacked histogram in panel A. For example, at 1000 ms, T1 is rarely presented (vertical distance that is dark blue) whilst there is an almost equal chance of presenting a T2 & T3 (vertical distances that are light blue & yellow, respectively). The distribution of lags between target stimuli is shown in panel B (blue histogram), alongside the probability of a miss occurring at any given lag (red line), where a miss here is defined as a cortical activation not followed by any binding pool activity. The proportion of misses per sequence of target stimuli is shown in panel C, which includes another type of miss: a binding pool activation that occurs at encoding but not at recall, indicating that little synaptic change with synfire chain groups took place. Having described the simulation procedure, we then go on to examine the timing mechanism of the model in panels D–G. Here, we show the local-field potential (LFP) of the faster dimensional synfire chain (D; green line), calculations shown in Appendix section 1.2, filtered by an α -function ($\tau = 15$ ms) & a 3–5Hz band-pass filter, which estimates the firing frequency of the synfire chain. This LFP was found to modulate several learning outcomes in the model. Firstly, it modulates the mean synaptic increase from any given synfire chain (SC) group to any active binding pool (BP) group (D; grey histogram), where a value of 1 indicates an all-to-all mapping and lower values indicate a weaker inter-group connection. Secondly, the LFP modulated the proportion of binding pool units that were active at encoding that are also active at recall (i.e. the “replay-ability” of the encoded binding, E; blue histogram), where a value of 1 indicates that all binding units that indexed a cortical event were also activated at recall, and lower values indicate a smaller proportion of those binding units were activated at recall. Lastly, the SC LFP negatively correlated with the reduced episodic distinctiveness (E; red histogram), described in Fig. 3, where a given binding might attach itself to sequential temporal positions (i.e. n SC binds = 2 in E; left-hand axis), which gives the false impression of a repetition at recall. This phenomenon can be shown to exist in anti-phase with the SC LFP (F), whilst the “replay-ability” of the encoded binding can be shown to exist in phase with the SC LFP (G). In the far-right hand panels (i–iii), we show the similarity (RSA) of phasic time series at encoding to recall for similar patterns (i.e. when the lags between T1, T2 & T3 were similar at encoding, i; red lines), to recall for different patterns (i.e. when the lags between T1, T2 & T3 were dissimilar at encoding, ii; black lines) and the content specificity across trials (i.e. similarity to same minus to different patterns, iii; pink lines). We do this for three conditions: for any sequence of target stimuli that contained at least one miss (i–iii; dotted lines, ≥ 1 miss); for any sequence with no misses, though a double SC binding occurs (i.e. “temporal smearing”, i–iii; dashed lines, > 1 binds); and finally for all other sequences (i.e. no misses or double SC binds, i–iii; solid lines, other). The purpose here is to highlight the effect that misses and mistakes have on the quality of the signal being decoded using the RSA approach.

similar is your signal to that of similar patterns relative to how similar it is to that for different patterns. We show here that for different patterns, where the lag between the target stimuli constitutes a bar-code like pattern, there is generally a positive content specific detection of the re-instatement of target patterns, followed by a smaller dip in detection performance (Fig. 6i–iv; grey shaded regions). We further break down our target patterns into those with varying lags between them, as defined by the vertical black lines in Fig. 6A–C (Fig. 6: i, lag ≤ 150 ; ii, $150 < \text{lag} \leq 300$; iii, $300 < \text{lag} \leq 600$; iv, $600 < \text{lag} \leq 1200$), which separate the behaviourally distinguishable regions described previously.

For small lags (Fig. 6i), it seems as though the high error-rates in encoding meant that the content specific detection of reinstated signatures was weak, where the similarity to the similar patterns is mostly weaker than that to different patterns. As 1–2 target stimuli are variably encoded (Fig. 6ii), this content specificity increases, though there is still some dissimilarity between similar and different patterns. Fig. 6iii highlights the sweet spot of this simulation procedure, when both target stimuli are successfully encoded and there is little stationarity in the signal between them, indicated by a consistently positive content specificity rating (pink line). However, as the lag between T1 & T2 increases and there is more stationarity in the identifying temporal signature (Fig. 6C; lag > 600 ms), there seems to be a much lower degree of similarity with different patterns (Fig. 6iv). Here, similarity also peaks when the convolved identifying signature perfectly aligns with the phasic signature of similar patterns at recall, otherwise it exists almost in perfect anti-phase to itself (indicated by the sinusoidal shape of the red line in Fig. 6iv). One can, for example, think of this as a binary 101 pattern convolving over a 000-101-000 pattern. This observation might be important for those considering using RSA in the reinstatement of temporal signatures, who might want to understand more about the neural code that might underlie the quality of the signal being decoded.

3.4. Oscillations enhance the episodic distinctiveness of memories

Next, we evaluate the timing mechanism of our model by reproducing many sequences of 3 randomly timed stimuli (Fig. 7). This allows us to consider the effect of the perceptual trade-off explained in Fig. 3, where a ramping up period of activation in our hierarchical synfire chains produces oscillatory down-phases that regulate temporal perception. This leads to the phasic modulation of both the quality and accuracy of bindings that are made. This allows us to examine the functional limitations of using oscillations to provide a temporal reference frame, as might occur in the brain (Barczak et al., 2019; Tai et al., 2020), where segregating perception into discernible chunks might actually improve the episodic distinctiveness of memories.

In evaluating the “timing” mechanism of our model, we initiate a similar simulation procedure as for evaluating the “binding” mechanism, though this time we introduce an additional target stimulus. In this way, we have initiated a T1, T2 & T3 sequence, where T1 occurs before T2 and T2 before T3. Aside from this, all stimulation times are random, where Fig. 7A shows the distribution of times for all target stimuli. As before, there is a binding punishment for a stimulus that occurs immediately after another stimulus, as indicated by Fig. 7B, where the probability a stimulus is missed negatively correlates with the lag between targets. Out of 2000 simulations, about 40% contained at least one missed stimulus (Fig. 7C). Some of these misses were not a binding issue, however, but a timing one. This is due to the ramping up nature of our hierarchical synfire chains, described in Fig. 4, which ultimately provides a sinusoidal segregation of time. Fig. 7D–G shows how the filtered synfire chain (SC) local field potential (LFP) modulates learning efficacy (Fig. 7D; grey histogram), binding pool “replay-ability” (Fig. 7E; blue histogram) and binding mistakes (Fig. 7E; red histogram). The modulation of weights bears some resemblance to the Theta modulated learning rule of our previous modelling work (Parish et al., 2018), where the intention was to create optimal phases of encoding, similar to experimental findings (Huerta and Lisman, 1995; Pavlides

et al., 1988). The “replay-ability” factor here is defined as the proportion of binding pool units that were active at encoding that are also active at retrieval. This gives us an indication of how many successful bindings were unable to be temporally contextualised by the oscillatory clock, due to them arriving during a down-phase.

One can appreciate the necessity of these oscillatory blind-spots when one considers the quality of encoded memory traces. Here, reduced episodic distinctiveness occur at a time when there is less weight change (Fig. 7D; grey histogram) that results in either a missed recall (Fig. 7E; blue histograms), or overlaps two consecutive synfire chain groups (Fig. 7E; red histograms, n SC binds = 2) to produce the false sense of a repetition at recall. When we analyse the content specific reinstatement of target memories, as we similarly did in Fig. 6, we see that sequences with multiple SC bindings were able to be recognised about as well as those with at least one miss in them (Fig. 7i–iii; multiple bindings shown as dashed lines, sequences with a miss shown as dotted lines, all other hits shown as a solid line. Similarity to similar sequences shown in red [i], similarity to different sequences shown in black [ii], and content specificity shown in pink [iii]). This indicates the role that oscillations might play in temporally segregating our episodic memories, providing clear windows that are optimal for learning (see Fig. 7G; where “replay-ability” is positively modulated by synfire chain phase), yet also segregate with down-phases to unambiguously discern sequential order more easily (see Fig. 7F; where multiple bindings is negatively modulated by synfire chain phase).

Previous research indicates that a cortical alpha desynchronisation and subsequent phase-reset patterns might signify information flow (Hanslmayr et al., 2012) and convey information content (Ng et al., 2013; Schyns et al., 2011), respectively. Here, we have shown some theoretical evidence for these findings, where a reduction in power (Fig. 4C; blue line) and phasic non-stationarity (Fig. 4C; red line) signifies the active representation of information (see also Fig. 7). Further, experimental evidence has suggested that one can decode information content through analysis of the phase-angle time series, enabling the identification of dynamic stimuli through examination of their unique temporal signatures (Michelmann et al., 2016). We have shown that this position can also be supported theoretically through the use of computational simulations. By presenting many unique temporal patterns to our model (Figs. 6 and 7), we can compare phasic signatures from encoding to retrieval between trials of the same pattern as well as to other patterns. Here, we use RSA to compare these phase-reset patterns (an example being given in Fig. 5K). The high degree of content specificity we observed, indicates that patterns were unique enough that on average, they did not resemble other patterns, and also that the phasic time-series of each pattern across trials was robust enough that on average, they resembled the same temporal signature. Taken together, the difference between these similarities can indicate the content specific reinstatement of unique temporal patterns. The lag in the reinstatement of these patterns can partly be attributed to the lag discussed in a previous paragraph, yet also resonates with the fact that the highest similarity occurs at the midpoint of comparable time-series (as seen in Figure 5L), which is further delayed for longer sequences (see Fig. 6i–iv; where the peak of content specificity moves according to the lag period being observed). The occasional dip in performance after content specific recognition, which is not present in the literature (Michelmann et al., 2016), seems to be due to the amount of stationarity in the identifying signature that is being convolved at recall. This means that as the pattern is convolved, the likelihood that the pattern exists in anti-phase to itself is higher. This is probably an unlikely occurrence in the brain due to the highly dynamic and complex representations that are active at any one time, and which are only observable as distributed and overlapping brain regions by non-specific methods such as EEG/MEG.

4. Discussion

We have here presented a novel neural network with three distinct mechanisms (see Fig. 1 for model architecture). We have shown how oscillations might facilitate the encoding and retrieval of episodic memories in a Sync/deSync framework (Hanslmayr et al., 2016; Parish et al., 2018). Here, oscillatory synchronisation enables communication and learning (Fell and Axmacher, 2011), whereas a desynchronisation indicates the active representation of information (Hanslmayr et al., 2012), which can further be decoded to decipher information content (Michelmann et al., 2016). This allows us to examine the quality of encoded episodes in relation to the interacting ensemble of our model. It was found that memories can be enhanced when oscillations are used to provide temporal reference frames (Lakatos et al., 2005), segregating episodic perception into discernible chunks. Encoding quality can also be diminished due to the limitations of binding within the model, which glues content together in time, such that events close together in time can be missed (Bowman and Wyble, 2007). Together, these mechanisms operate in harmony to enable us to bind discrete, observable events in time, though each mechanism allows us to explore a distinct set of hypotheses.

4.1. On examining the quality of neo-cortical representations

We first instantiate a neo-cortical (NC) mechanism (Fig. 1A), where intrinsic oscillations are generated at a resting alpha frequency through recurrent excitatory-inhibitory interactions. Here, we have implemented a winner-take-all mechanism in a “Mexican-hat” like topology, as has also been described in hierarchical models of vision, recognition and attention (Carpenter and Grossberg, 1987; Itti et al., 1998; Reisenhuber and Poggio, 1999). By introducing an external event to our NC region, a subset of winning units that coded for that specific stimulus remained active whilst others were silent. During this time, the intrinsic frequency was de-synchronised (Fig. 4Ai), consistent with the experimental hypothesis that oscillatory desynchronisations are due to increased neural activation (Haegens et al., 2011; Hanslmayr et al., 2011a), which occurs due to relevant representations becoming active at the expense of others (Hanslmayr et al., 2012). However, in Fig. 6 we found that this competitive framework produced an effect that was more pronounced than typically observed in the “attentional-blink” paradigm. Here, the first of two target stimuli (the T1), had a substantially reduced accuracy if the second target stimulus (the T2) was presented around the same time, an effect observed in traditional “attentional-blink” paradigms (Bowman and Wyble, 2007), but typically more weakly. This is due to the “Mexican-hat” topology of the simulated network, in particular when we instead used repeating stimuli (Fig. 6A; dashed line, a T1 repetition, i.e. where there was no competition in representations), T1 accuracy for short lags was high. This resembles experimental findings where a reduced T1 blink was observed for stimuli where the T1 and T2 shared some content or overlapping neural representations (Lindh et al., 2019).

The degree to which spikes conform to the local field potential is not fully explored here. We have instantiated a population with a high degree of spike uniformity to the alpha rhythm, though this is likely not the case for a typical cortical population (Chapeton et al., 2019). We anticipate that the degree of cortical spike coherence to alpha does not impact learning very much in our model, which is simply generated by stimulus locked neural activity, not alpha specifically. The impact would most likely be felt in the ability of a higher function or external observer to “read” the unique phasic signature that arises from underlying neural firing relative to the alpha rhythm, as deviations in neural firing become indistinguishable from the increasingly non-uniform background. Whilst further theoretical work can still be undertaken to determine the level of spike uniformity required to be able to decipher memories in such a manner, this work is more focused with the encoding and reactivation of entire episodic memories. Any experimental work on this

issue would help us to further constrain our parameters for this aspect of our model.

The model described here was built on previous modelling work (Parish et al., 2018), where a cortical desynchronisation signified general information processing as content was being represented and reinstated. Recently, experimental evidence suggested that one can decode more than general signals of processing from cortical alpha oscillations, where phasic patterns are thought to convey information content (Ng et al., 2013; Schyns et al., 2011). Here, one can even identify a stimulus by a unique temporal signature that can be used to later detect its re-instatement in memory (Michelmann et al., 2016; Michelmann et al., 2018; Michelmann et al., 2019), a method that has also been applied in several recent MEG studies (Kornysheva et al., 2019; Kurth-Nelson et al., 2016; Lui et al., 2019). In order to theoretically explore the neural mechanisms underlying such a phasic code, it was important to add a temporal dynamic to our model. In doing so, we expanded upon the simple cosine wave that dictated phasic information of previous modelling work (Parish et al., 2018), by implementing a feedback network of excitatory and inhibitory neurons (see Fig. 1). This allowed the phase of the population to be dictated by internally generated population dynamics, further allowing an external stimulation to trigger a phase-reset of the intrinsically generated oscillation. We explored this dynamic in Fig. 4, where a stimulation of varying length was presented to the cortical network at various phases of the internally generated frequency. Stimuli that occurred during the peak of the entraining oscillation did not cause a phase-reset, and indeed caused a small synchronisation in the power spectrum. This aligns with experimental evidence where phase locking of transcranial magnetic stimulation (TMS) bursts occurred as a function of pre-stimulation alpha phase (Thut et al., 2011). This indicates that internally generated alpha phase gates the representation of stimuli, a theory known as the “inhibition-timing” hypothesis (Klimesch et al., 2007). We also show here that a desynchronisation of the frequency can be used to identify whether a stimulus was able to surpass the gating mechanism of local inhibitory circuits, where desynchronisation occurred as a function of phase (Fig. 4D). Indeed, desynchronisation negatively correlates with the form of the recurrent inhibitory α -function that after a small delay, follows excitatory activity during the peak.

Here, we simulate a single cortical population, with lateral competition within the local circuitry. In future works, we would like to increase this in scale to incorporate many such populations. Other models have found that several regions, each with an independent intrinsic oscillation, can align in phase through the mediation of a coordinating pacemaker (Vicente et al., 2008). As this is a proposed mechanism through which independent cortical columnal alpha oscillators are thought to align in phase, possibly through recurrent thalamo-cortical loops, it would be of further interest to instantiate a similar environment and assess whether phase can be robustly used to convey information content. One could then also explore whether a priming event might cause a general phase-reset in thalamo-cortical columns, as has been hypothesised to occur during the P1 ERP component (~110 ms) of general recognition (Hanslmayr et al., 2011b). This might ensure that cortical regions are pre-aligned in phase and thus optimally entrained to a given stimulus. Then any subsequent phase-reset patterns might be more consistent across trials and not as reliant on initial intrinsically generated oscillatory conditions. This larger scale model would also allow us to encode multiple trace memories, where cortical content would be more distributed across several populations rather than competing within a single one, perhaps leading to a more identifiable phase-reset signature.

Episodic memories have an inherent temporal dynamic. Studies have suggested that our perception is not continuous but is rhythmically sampled in discrete alpha-frequency time-steps (Hanslmayr et al., 2013; Landau and Fries, 2012; VanRullen et al., 2007). It might therefore be the case that there is a more qualitative element to alpha desynchronisations. As neocortical and hippocampal gamma oscillations have both

been found to be important when predicting successful memory encoding (Sederberg et al., 2007), it might be the case that an alpha desynchronisation deregulates alpha-frequency inhibition in order for a gamma-frequency sequence to be allowed to activate. In this sense, our neocortex within the model might undergo learning to inherit a hippocampal sequence during encoding (or more likely, during sleep), as other models have shown is possible (Itskov et al., 2011), even in the absence of a downstream feed-forward architecture. The deregulation of alpha inhibition might then enable the inherited cortical sequence to play in full, both decreasing alpha power and increasing respective gamma power.

4.2. On the discrete indexing of events using a binding pool

The second mechanism within our model (Fig. 1B) ensured that events were treated discretely such that they could be bound as independent components of a sequence, similar to other models of ordinal working memory (Bowman and Wyble, 2007). Verification of the existence of such “index” cells, possibly in the medial-temporal-lobe (Squire et al., 2004). Through our explorations, we predict that the bursting of single cells is an essential component of this indexing process, an observation also made when inducing plasticity in hippocampal cell cultures (Huerta and Lisman, 1995), where a single burst can be sufficient for long term plasticity (Ison et al., 2015).

We here argue that the use of a binding-pool enables the encoding of repetitions when employing a hierarchical representation of time (see Fig. 3), as might be the case if nested oscillatory frequencies are considered to aid selectivity in attention (Lakatos et al., 2008) and stimulus processing (Schroeder and Lakatos, 2009) by providing a temporal reference frame (Tai et al., 2020). Perhaps this then speaks for the necessity of discretisation, thought to occur in the medial temporal lobe (Squire, 1992; Squire et al., 2004) as part of the CLS framework (McClelland et al., 1995; O’Reilly et al., 2011). One might then consider this framework to have evolved into a steady-state, where the length of activation of any given discretised binding would be shorter than the down-phase of any oscillatory temporal reference frame, lest a conjunction between multiple competing reference frames occurs (see Fig. 3D and E). An investigation into the existence of these specific forms of temporal conjunction errors would give more insight into the brain’s adherence to a hierarchical and oscillatory discretisation of time. Alternatively, considering that a repetition seems to induce a “jump-back in time” in human MTL neurons (Howard et al., 2012), an argument might be made that the brain is not so tolerant towards repetition induced binding errors such as these, and thus might not discretise events in the manner of our binding pool.

An interesting phenomenon exhibited by the model is the effect of the “off switch” mechanism in the binding pool that operates to prevent spreading activation across the excitatory population (see Fig. 1 for description). It was found that a new event would not be encoded during this inhibitory pulse, as cortical impulses could not overcome the increased global inhibition (see Fig. 6; for analysis of binding accuracy of two target stimuli close together in time). This is reminiscent of the hypothesised function of binding in other models (Bowman and Wyble, 2007), where it is thought that attentional deficits for events very close together in time arise as a consequence of the need to limit the temporal extent of the binding process (Wyble et al., 2011). In our model, it is sufficient that the synaptic time constant from the “off-switch” cells to excitatory cells merely match that between excitatory cells (in Fig. 6B; this is the black dashed line, $\tau = 5$ ms). This would then quench the possibility that activation escalates out of control. However, this time constant might be larger to further minimise binding errors, as well as acting in its default role of preventing runaway activity (Bowman and Wyble, 2007; Swan and Wyble, 2014). This might especially be necessary when encoding over very fine-grained temporal dimensions, where a global inhibitory pulse could be useful in separating events close

together in time, though it risks causing an attentional blink for those events that follow before inhibition subsides. In our model, we varied the parameter that dictates the depth and length of this attentional blink (see Fig. 6B; varying the time constant for binding pool $O \rightarrow E$ synapses), indicating how the brain’s mechanism to maintain network stability might have been adapted to separate events into distinguishable episodes, where a balance between network stability and minimising attentional costs evolves over generations. If these two functions were indeed intrinsically linked, then one might expect to see this attentional deficit correlate with individual differences in levels of inhibition.

Our model also allowed for multiple events to be encoded within the same binding, as shown in Fig. 6A and B, where binding pool capacity was only reduced by the amount of a single binding yet both target stimuli were invariably encoded. This echoes the “illusion of integration” finding (Simione et al., 2017), where it was found that when illusory conjunctions of a T1 and T2 could create a meaningful integrated percept, that percept was subjectively experienced similarly well as a T1 on its own. The lower T1 accuracy here parallels the existence of order errors when reactivating these events later, as has also been found in the literature for the encoding of events close together in time (Wyble et al., 2009). We also analyse the stationarity and synchronicity of the cortical intrinsic oscillation in these instances (Fig. 6C), showing that neural representations at recall only slightly increased in quality for two target stimuli at low lags. It would be good to further investigate the link between cortical oscillatory stability and the lag between target stimuli in line with other research, where overlapping representations were found to have an effect on the attentional blink (Lindh et al., 2019). This could be achieved by expanding on the number of cortical populations and creating more distributed representations. It would also be interesting to link our broadly tuned binding pool, likely hippocampal in origin, with the adaptive coding theory of the prefrontal cortex (Duncan, 2001), where very broadly tuned units were also found. Here, one might theoretically explore how communication between these regions enables and maintains the adaptive coding of tasks and stimuli. In sum, we here argue for the existence of a binding pool in episodic memory formation by correlating the occurrence of an attentional-blink phenomenon in our model to that which is well documented in the literature (Botella et al., 1992; Bowman and Wyble, 2007; Swan and Wyble, 2014; Wyble et al., 2009). Due to the abstractedness of content representation in our model, we cannot make claims as to the modality of the stimuli involved. We show here how events occurring very close together in time have a lower chance of being encoded, and thus also failing to be retrieved from memory. The novelty of our analysis lies in relating these attentional demands on memory to alpha oscillations, where we predict that alpha power and stationarity should track the number of items that were successfully encoded (see Fig. 6C). Therefore, it might be possible to detect if attentional demands have inhibited memory performance through analysing electrophysiological time series.

4.3. On hierarchical and oscillatory temporal reference frames

Our primary motivation for the third component of our model is to explore how nested oscillatory frequencies might provide a temporal reference frame for selective stimulus processing (Barczak et al., 2019; Lakatos et al., 2005; Schroeder and Lakatos, 2009; Tai et al., 2020). If we are to consider the binding of memories as a spike-timing-dependent plasticity (STDP) process (Markram et al., 1997; Boo and Poo, 2001), where neural populations that are concurrently active bind together to encode new information (Hebb, 1949), then a plausible framework for such a temporal referencing schema would be transiently active cell assemblies. These are typically implemented as synfire chains, groups of consecutively connected cell assemblies (Diesmann et al., 1999), which are thought to naturally occur (Kumar et al., 2008; Fiete et al., 2010) and contribute to the precise transmission of information across the brain (Mauk and Buonomano, 2004). One such implementation of synfire chains (Itskov et al., 2011) has been shown to produce time-cell

behaviour consistent with that observed in the rat hippocampus (MacDonald et al., 2013), which is thought to aid the temporal mapping of memories (Eichenbaum, 2014). However, such chains are thought unlikely to encode for the long temporal durations required of human episodic memory (Shankar and Howard, 2012), due to the length of the chain having to increase linearly with time. In the current modelling work, we show in Fig. 2B how discretising temporal encoding in such a feedforward manner is much more efficient if the chains are hierarchical. Akin to another recent model of hierarchical time-ramping cells (Rolls and Mills, 2019) found in the entorhinal cortex (Tsao et al., 2018), we have aimed here to implement a novel instantiation of hierarchical synfire chains (see Fig. 2) that encodes for multiple temporal scales (Howard and Eichenbaum, 2013). Our contribution here then, is to have used such a representation of time in the wholesale encoding and reactivation of an episodic memory trace, as observed in human EEG signals (Michelmann et al., 2016). In doing so, we postulate that the ramping up nature of hierarchical chains, modelled here as elsewhere (Rolls and Mills, 2019), might serve the functional purpose of aiding the episodic distinctiveness of memories by providing buffers of suboptimal binding (see Figs. 2B & 7). This, then, is relatable to the nested oscillatory hierarchies found in stimulus processing (Lakatos et al., 2005), that are thought to aid selectivity in attentional (Lakatos et al., 2008) and sensory processing (Schroeder and Lakatos, 2009), possibly by providing temporal reference frames (Barczak et al., 2019; Tai et al., 2020). In making this relation, we have shown how a transiently active, feed-forward and oscillatory cell assembly can modulate the quality of memories (see Fig. 7), and possibly learning more generally (Hasselmo et al., 2002), if they were employed in maintaining oscillatory reference frames for episodic memory. A question that arises then, is whether such a temporal reference mechanism is central to the MTL, as has been found in the examination of time-ramping cells in the rat MTL (MacDonald et al., 2013; Tsao et al., 2018), or whether they are more distributed across the cortex, enabling enhanced selectivity in attentional (Lakatos et al., 2008), sensory (Schroeder and Lakatos, 2009) and stimulus processing (Lakatos et al., 2005), all of which are key for human episodic memory.

As such, one neural substrate contender for our timing mechanism might be that it resides in the entorhinal cortex, corresponding to time-ramping cells, as in similar models (Rolls and Mills, 2019), or even in hippocampal CA1 as intrinsic sequences, as another theory has suggested (Cheng, 2013). In this case, time-keeping would be centralised and disseminated to sensory processing brain regions (Church, 1984). As an alternative neural substrate contender, local subsystems might produce their own time-keeping (Mauk and Buonomano, 2004), perhaps inducing the nested oscillatory hierarchies implicated in stimulus processing in the auditory cortex (Lakatos et al., 2005). Thus, their distributed placement here would be made all the more feasible by using a hierarchical rather than one-dimensional discretisation, as shown in Fig. 2. Though the nature of our time-keeping mechanism might alternatively arise from heteroclinic synchronisation (i.e. synchronisation between two equilibria of a continuous time dynamical system, where a weak periodic input is thought to synchronise low-frequency oscillations, Rabinovich, et al., 2006), membrane resonance (Hutcheon et al., 1996), or any other such means, we hope here to have contributed to the theoretical use of such a hierarchical discretisation of time, which allows us to encode the absolute distance between the beats and pauses of human episodic memory traces (Michelmann et al., 2016).

Adaptations of hierarchical time-keeping mechanisms might enable a signal to traverse chains at varying speeds depending upon the strength of the initial burst or levels of background noise, as other feedforward synfire models have explored (Diesmann et al., 1999; Kumar et al., 2008). In this way, one could reactivate events at a faster rate, as has been observed during sleep (Diekelmann and Born, 2010). It might also be the case that some attentional mechanism can skip through scene-sized chunks, as indicated by recent findings (Michelmann et al., 2019), where selective additional excitatory input focussed on a specific

temporal dimension might compress memory reactivation until a point of interest is identified through an additional event-driven feedback mechanism. As well as this temporal compression, the mechanism might also be adapted to allow for reactivation to occur in reverse, as has been found for human time cell sequences (Eichenbaum, 2014). Of further interest would be to restart chains from content-specific locations, in order to kickstart episodic memory traces from specific locations.

Considering the degree to which the temporal structure proposed here can condense a long and complex representation of time onto a relatively small neuronal population, we anticipate that it is compatible with both a centralised and distributed encoding of time (Mauk and Buonomano, 2004), where time is either broadcast from a central location (possibly from the medial-temporal-lobe [MTL]) or is distributed across cortical populations. Therefore, if MTL were damaged and temporal replay were not hampered, then it might be strong evidence that these chains exist in a more distributed fashion. If, following MTL damage, new sequences were also not encoded, then this might suggest that temporal sequences originate in the MTL, then migrate to distributed regions in a one-to-one mapping to be stored as long-term memories, as a recent model has shown is possible (Itskov et al., 2011). It appears that the brain facilitates sequential and temporal processing over shorter timescales, without requiring the MTL (Mauk and Buonomano, 2004). This more distributed timekeeping might arise as an emergent property of a dynamical system (Mauk and Buonomano, 2004). Another suggestion in line with the modelling work presented here, is that this might be achieved through the brain's preference for synfire chains (Fiete et al., 2010), which help to facilitate high speed and accurate communication (Diesmann et al., 1999) – and perhaps, temporal processing. As one of the first models to encode and replay complete episodic memory traces, we hope to stimulate further theoretical work on understanding how the brain accurately processes temporal information, over short and long timescales.

Though the paradigm we have simulated is rather simple, we can speculate as to what might occur in more complex paradigms by examining the three components of our model. For example, what would happen if two sequences made up of stimuli ABCD were played with variable inter stimulus intervals. Firstly, we can think of each stimulus as occupying a region of cortical space, activating the same neuronal population with each occurrence. Next, the binding pool will encode each repetition of content as a unique occurrence, enabling the differentiation of the same note occurring multiple times in a sequence, or in multiple sequences. If we then decide to cue with stimulus A, then one would have to first enable binding to synfire chain LTP. In this way, cortical to binding activation would induce the synfire chains to begin from the moment stimulus A was encoded. As there are multiple sequences associated with stimulus A, then the model will have to choose which sequence to play. This would be achieved by the lateral inhibition of the binding pool, which would ensure that only one binding pool group could be active at any one time. This “decision” could be influenced in a number of ways not modelled here, such as feedback from cortical regions, emotional salience, etc. The strength of the division of labour that we describe here lies in the ability to temporally contextualise repeating content, where each component works independently yet in unison to together index the occurrence of repeating content at a particular moment in a temporal sequence.

As oscillations are an intrinsic part of our model, we might further speculate as to the consequence of their reduction in amplitude, for example, by a pharmacological agent. We regard alpha oscillations as gateways to content representation, where stronger baseline alpha oscillations would entail higher informational capacity as stimulated regions signal content activation by desynchronising out of the entraining rhythm (Hanslmayr et al., 2012). Thus, in our model, a stronger alpha would both inhibit the emergence of weaker stimuli occurring on down-phases of alpha (as we have shown in Fig. 4) and increase the reliability of deciphering information content based on alpha phase, and vice versa for a weaker alpha. As for nested frequencies within this

model, we speculate that a contributing factor to their emergence might be the coactivation of hierarchical sequences that together, can provide unique temporal reference frames. If these were somehow reduced in amplitude, then one might expect that the ability to differentiate between stimuli in a sequence might be compromised, both at encoding and retrieval.

5. Conclusion

In conclusion, we have here presented a neural network model to examine a set of theoretical mechanisms that might enable the accurate encoding and reactivation of dynamic episodic memory traces. These being: that a deregulation of cortical alpha phase can be interpreted to consistently identify information content; that a discrete indexing of events is necessary to contextualise overlapping or repeating components of a memory; and that nested frequencies are a cost-effective solution to the provision of reference frames for temporal sequences. In doing so, we hope to stimulate further discussion that takes a holistic approach towards human episodic memory.

Credit author statement

George Parish: Conceptualisation, Investigation, Writing – original draft. Sebastian Michelmann: Methodology, Writing – review & editing. Simon Hanslmayr: Supervision, Writing – review & editing. Howard Bowman: Supervision, Writing – review & editing.

Declaration of competing interest

None.

Appendix A. Supplementary data

Supplementary data to this article can be found online at <https://doi.org/10.1016/j.neuropsychologia.2021.107867>.

References

- Barczak, A., et al., 2019. Dynamic modulation of cortical excitability during visual active sensing. *Cell Rep.* 27, 3447–3459.
- Barnard, P., 2002. Mapping neural architecture to mental architecture and mental architecture to behavioural architecture. <https://doi.org/10.13140/RG.2.2.36214.14401> [Online] Available at:
- Boo, G., Poo, M., 2001. Synaptic modification by correlated activity: hebb's postulate revisited. *Annu. Rev. Neurosci.* 24 (1), 139–166.
- Botella, J., Garcia, M.L., Barriopedro, M., 1992. Intrusion patterns in rapid serial visual presentation tasks with two response dimensions. *Percept. Psychophys.* 52 (5), 547–552.
- Bowman, H., Wyble, B., 2007. The simultaneous type, serial token model of temporal attention and working memory. *Psychol. Rev.* 114 (1), 38–70.
- Brown, G.D., Preece, T., Hulme, C., 2000. Oscillator-based memory for serial order. *Psychol. Rev.* 107 (1), 127–181.
- Brunel, N., 2000. Dynamics of sparsely connected networks of excitatory and inhibitory spiking neurons. *J. Comput. Neurosci.* 8, 183–208.
- Buzsáki, G., 2002. Theta oscillations in the Hippocampus. *Neuron* 33, 325–340.
- Canavier, C.C., 2015. Phase-resetting as a tool of information transmission. *Curr. Opin. Neurobiol.* 31, 206–213.
- Carpenter, G.A., Grossberg, S., 1987. A massively parallel architecture for a self-organizing neural pattern recognition machine. *Comput. Vis. Graph Image Process* 37 (1), 54–115.
- Chapeton, I.J., et al., 2019. Large-scale communication in the human brain is rhythmically modulated through alpha coherence. *Curr. Biol.* 29 (17), 2801–2811.
- Cheng, S., 2013. The CRISP theory of hippocampal function in episodic memory. *Front. Neural Circ.* 7 (88), 1–14.
- Chennu, S., Bowman, H., Wyble, B., 2011. Fortunate conjunctions revived: feature binding with the 2f-ST2 model. *Proc. Ann. Meet. Cognit. Sci. Soc.* 33 (33).
- Chun, M.M., Potter, M.C., 1995. A two-stage model for multiple target detection in rapid serial visual presentation. *J. Exp. Psychol. Hum. Percept. Perform.* 21 (1), 109.
- Church, R.M., 1984. Properties of the internal clock. *Ann. N. Y. Acad. Sci.* 423 (1), 566–582.
- Diekelmann, S., Born, J., 2010. The memory function of sleep. *Nat. Rev.* 11 (2), 114–126.
- Diesmann, M., Gewaltig, M.-O., Aertsen, A., 1999. Stable propagation of synchronous spiking in cortical neural networks. *Nature* 402, 529–533.
- Duncan, J., 2001. An adaptive coding model of neural function in prefrontal cortex. *Nat. Rev.* 2, 820–829.
- Eichenbaum, H., 2014. Time cells in the hippocampus: a new dimension for mapping memories. *Nat. Rev.* 15, 732–744.
- Fell, J., Axmacher, N., 2011. The role of phase synchronisation in memory processes. *Nat. Rev. Neurosci.* 12, 105–118.
- Fell, J., et al., 2011. Medial temporal theta/alpha power enhancement precedes successful memory encoding: evidence based on intracranial EEG. *J. Neurosci.* 31 (14), 5392–5397.
- Fiete, I., Senn, W., Wang, C., Hahnloser, R., 2010. Spike-time-dependent plasticity and heterosynaptic competition organize networks to produce long scale-free sequences of neural activity. *Neuron* 65 (4), 563–576.
- Fries, P., 2005. A mechanism for cognitive dynamics, neuronal communication through neuronal coherence. *Trends Cognit. Sci.* 9, 474–480.
- Fries, P., 2015. Rhythms for cognition: communication through coherence. *Neuron* 88, 220–235.
- Friston, K., et al., 2018. Deep temporal models and active inference. *Neurosci. Biobehaviour. Rev.* 90, 486–501.
- Goldman, M.S., 2009. Memory without feedback in a neural network. *Neuron* 61, 621–634.
- Graupner, M., Brunel, N., 2012. Calcium-based plasticity model explains sensitivity of synaptic changes to spike pattern, rate, and dendritic location. *Proc. Natl. Acad. Sci. Unit. States Am.* 109 (10), 3991–3996.
- Griffiths, B.J., et al., 2019. Directional coupling of slow and fast hippocampal gamma with neocortical alpha/beta oscillations in human episodic memory. *Proc. Natl. Acad. Sci. Unit. States Am.* 116 (43), 21834–21842.
- Haegens, S., et al., 2011. α -Oscillations in the monkey sensorimotor network influence discrimination performance by rhythmical inhibition of neuronal spiking. *Proc. Natl. Acad. Sci. Unit. States Am.* 108 (48), 19377–19382.
- Hanslmayr, S., Gross, J., Wolfgang, K., Shapiro, K., 2011b. The role of alpha oscillations in temporal attention. *Brain Res. Rev.* 331–343.
- Hanslmayr, S., Staresina, B.P., Bowman, H., 2016. Oscillations and episodic memory: addressing the synchronization/desynchronization conundrum. *Trends Neurosci.* 39 (1), 16–25.
- Hanslmayr, S., Staudigl, T., 2014. How brain oscillations form memories - a processing based perspective on oscillatory subsequent memory effects. *Neuroimage* 85, 648–655.
- Hanslmayr, S., Staudigl, T., Fellner, M.-C., 2012. Oscillatory power decreases and long-term memory: the information via desynchronization hypothesis. *Front. Hum. Neurosci.*
- Hanslmayr, S., et al., 2013. Prestimulus Oscillatory Phase at 7 and Hz Gates Cortical Information Flow Visual Perception. *Curr Biol*, vol. 23. Elsevier Ltd, pp. 2273–2278.
- Hanslmayr, S., Volberg, G., Wimber, M., Raabe, K.-H.T., 2011a. The relationship between brain oscillations and BOLD signal during memory formation: a combined EEG-fMRI study. *J. Neurosci.* 31, 15674–15680.
- Hasselmo, M.E., Bodelon, C., Wyble, B.P., 2002. A proposed function for hippocampal theta rhythm: separate phases of encoding and retrieval enhance reversal of prior learning. *Neural Comput.* 14 (4), 793–817.
- Hebb, D., 1949. *The Organization of Behaviour: A Neuropsychological Theory*. John Wiley and Sons, Inc, New York.
- Hodgkin, A.L., Huxley, A.F., 1952. A quantitative description OF membrane current and its application to conduction and excitation IN nerve. *J. Physiol.* 117, 500–544.
- Howard, M., Viskontas, W., Shankar, K.H., Fried, I., 2012. Ensembles of human MTL neurons “jump back in time” in response to a repeated stimulus. *Hippocampus* 22, 1833–1847.
- Howard, W.M., Eichenbaum, H., 2013. The Hippocampus, time, and memory across scales. *J. Exp. Psychol.* 142 (4), 1211–1230.
- Huerta, P.T., Lisman, J.E., 1995. Bidirectional synaptic plasticity induced by a single burst during cholinergic theta oscillation in CA1 in vitro. *Neuron* 1053–1063.
- Hutcheon, B., Miura, R.M., Putil, E., 1996. Subthreshold membrane resonance in neocortical neurons. *J. Neurophysiol.* 76 (2), 683–697.
- Ison, M.J., Quiroga, R.Q., Fried, I., 2015. Rapid encoding of new memories by individual neurons in the human brain. *Neuron* 87, 220–230.
- Itskov, V., Curto, C., Pastalkova, E., Buzsáki, G., 2011. Cell assembly sequences arising from spike threshold adaptation keep track of time in the Hippocampus. *J. Neurosci.* 31 (8), 2828–2834.
- Itti, L., Koch, C., Niebur, E., 1998. A model of saliency-based visual attention for rapid scene analysis. *IEEE Trans. Pattern Anal. Mach. Intell.* 20 (11), 1254–1259.
- Jensen, O., Idiart, M., Lisman, J., 1996. Physiologically Realistic Formation of Autoassociative Memory in Networks with Theta/Gamma Oscillations: Role of Fast NMDA Channels. *Learning & Memory*, pp. 243–256.
- Jensen, O., Mazaheri, A., 2010. Shaping functional architecture by oscillatory alpha activity: gating by inhibition. *Front. Hum. Neurosci.* 4 (186).
- Khader, P., Jost, K., Ranganath, C., Rosler, F., 2010. Theta and Alpha oscillations during working-memory maintenance predict successful long-term memory encoding. *Neurosci. Lett.* 468 (3), 339–343.
- Klimesch, W., Barbel, S., Sauseng, P., 2005. The functional significance of theta and upper alpha oscillations. *Exp. Psychol.* 52 (2), 99–108.
- Klimesch, W., Sauseng, P., Hanslmayr, S., 2007. EEG alpha oscillations: the inhibition–timing hypothesis. *Brain Res. Rev.* 53 (1), 63–68.
- Kornysheva, K., et al., 2019. Neural competitive queuing of ordinal structure underlies skilled sequential action. *Neuron* 101 (6), 1166–1180.
- Kumar, A., Rotter, S., Aertsen, A., 2008. Conditions for propagating synchronous spiking and asynchronous firing rates in a cortical network model. *J. Neurosci.* 28 (20), 5268–5280.

- Kurth-Nelson, Z., Economides, M., Dolan, R., Dayan, P., 2016. Fast sequences of non-spatial state representations in humans. *Neuron* 91 (1), 194–204.
- Lakatos, P., et al., 2008. Entrainment of neuronal oscillations as a mechanism of attentional selection. *Science* 80, 110–113.
- Lakatos, P., et al., 2005. An oscillatory hierarchy controlling neuronal excitability and stimulus processing in the auditory cortex. *J. Neurophysiology* 94, 1904–1911.
- Landau, A., Fries, P., 2012. Attention Samples Stimuli Rhythmically, vol. 22. *Curr Biol.* Elsevier Ltd, pp. 1000–1004.
- Lindh, D., et al., 2019. Conscious perception of natural images is constrained by category-related visual features. *Nat. Commun.* 10 (4106).
- Lisman, J.E., Jensen, O., 2013. The theta-gamma neural code. *Neuron* 77 (6), 1002–1016.
- Lui, Y., Dolan, R., Kurth-Nelson, Z., Behrens, T., 2019. Human replay spontaneously reorganizes experience. *Cell* 178 (3), 640–652.
- MacDonald, C.J., Carrow, S., Place, R., Eichenbaum, H., 2013. Distinct hippocampal time cell sequences represent odor memories in immobilized rats. *J. Neurosci.* 33, 14607–14616.
- Markram, H., Lübke, J., Frotscher, M., Sakmann, B., 1997. Action potentials propagating back into dendrites triggers changes in efficacy. *Science* 275 (5297), 213–215.
- Mauk, M.D., Buonomano, D.V., 2004. The neural basis of temporal processing. *Annu. Rev. Neurosci.* 27, 307–340.
- McClelland, J., McNaughton, B., O'Reilly, R., 1995. Why there are complementary learning systems in the hippocampus and neocortex: insights from the successes and failures of connectionist models of learning and memory. *Psychol. Rev.* 102, 419–457.
- McCloskey, M., Cohen, N.J., 1989. Catastrophic Interference in Connectionist Networks: the Sequential Learning Problem, vol. 24. Elsevier, pp. 109–165.
- Michelmann, S., Bowman, H., Hanslmayr, S., 2016. The temporal signature of memories: identification of a general mechanism for dynamic memory replay in humans. *PLoS Biol.* 14 (8).
- Michelmann, S., Bowman, H., Hanslmayr, S., 2018. Replay of stimulus-specific temporal patterns during associative memory formation. *J. Cognit. Neurosci.* 30 (11), 1577–1589.
- Michelmann, S., Staresina, B., Bowman, H., Hanslmayr, S., 2019. Speed of time-compressed forward replay flexibly changes in human episodic memory. *Nat. Human Behav.* 3 (2), 143.
- Ng, B., Logothetis, N., Kayser, C., 2013. EEG phase patterns reflect the selectivity of neural firing. *Cerebr. Cortex* 23, 389–398.
- O'Reilly, R., Bhattacharyya, R., Howard, M., Ketz, N., 2011. Complementary Learning Systems. *Cognitive Science*, pp. 1–20.
- O'Reilly, R.C., Munakata, Y., 2000. *Computational Explorations in Cognitive Neuroscience*. s.l. MIT Press.
- Parish, G., Hanslmayr, S., Bowman, H., 2018. The Sync/deSync model: how a synchronized Hippocampus and a desynchronized neocortex code memories. *J. Neurosci.* 38 (14), 3428–3440.
- Pavlidis, C., Greenstein, Y., Grudman, M., Winson, J., 1988. Long-term potentiation in the dentate gyrus is induced preferentially on the positive phase of θ -rhythm. *Brain Res.* 493 (1–2), 383–387.
- Rabinovich, M.I., Huerta, R., Varona, P., 2006. Heteroclinic synchronization: ultrasubharmonic locking. *Phys. Rev. Lett.* 96.
- Raymond, J.E., Shapiro, K.L., Arnell, K.M., 1992. Temporary suppression of visual processing in an RSVP task: an attentional blink? *J. Exp. Psychol. Hum. Percept. Perform.* 18 (3), 849.
- Reisenhuber, M., Poggio, T., 1999. Hierarchical models of object recognition in cortex. *Nat. Neurosci.* 2, 1019–1025.
- Rolls, T.E., Mills, P., 2019. The generation of time in the hippocampal memory system. *Cell Rep.* 28, 1649–1658.
- Schreiner, T., et al., 2018. Theta phase-coordinated memory reactivation reoccurs in a slow-oscillatory rhythm during NREM sleep. *Cell Rep.* 25 (2), 296–301.
- Schroeder, C.E., Lakatos, P., 2009. Low-frequency neuronal oscillations as instruments of sensory selection. *Trends Neurosci.* 32, 9–18.
- Schyns, P., Thut, G., Gross, J., 2011. Cracking the code of oscillatory activity. *PLoS Biol.* 9.
- Sederberg, P.B., et al., 2007. Hippocampal and neocortical gamma oscillations predict memory formation in humans. *Cerebr. Cortex* 17, 1190–1196.
- Shankar, K., Howard, M., 2012. A scale-invariant internal representation of time. *Neural Comput.* 24, 134–193.
- Simione, L., et al., 2017. Illusions of Integration Are Subjectively Impenetrable: Phenomenological Experience of Lag 1 Percepts during Dual-Target RSVP, vol. 51. *Consciousness and Cognition*, pp. 181–192.
- Squire, L.R., 1992. Memory and the Hippocampus: a synthesis from findings with rats, monkeys, and humans. *Psychol. Rev.* 99 (2), 195–231.
- Squire, L.R., Stark, C.E.L., Clark, R.E., 2004. The medial temporal lobe. *Annu. Rev. Neurosci.* 27, 279–306.
- Staresina, B.P., et al., 2016. Hippocampal pattern completion is linked to gamma power increases and alpha power decreases during recollection. *eLife* 5, e17397.
- Staudigl, T., Hanslmayr, S., 2019. Reactivation of neural patterns during memory reinstatement supports encoding specificity. *Cognit. Neurosci.* 10 (4), 175–185.
- Staudigl, T., Vollmar, C., Noachtar, S., Hanslmayr, S., 2015. Temporal-pattern similarity analysis reveals the beneficial and detrimental effects of context reinstatement on human memory. *J. Neurosci.* 35, 5373–5384.
- Swan, G., Wyble, B., 2014. The binding pool: a model of shared neural resources for distinct items in visual working memory. *Atten. Percept. Psychophys.* 76, 2136–2157.
- Tai, I., Leszczynski, M., Mesgarani, N., Schroeder, C.E., 2020. Does the phase of ongoing EEG oscillations predict auditory perception? *bioRxiv*.
- Thut, G., et al., 2011. Rhythmic TMS causes local entrainment of natural oscillatory signatures. *Curr. Biol.* 21 (14), 1176–1185.
- Tsao, A., et al., 2018. Integrating time from experience in the lateral entorhinal cortex. *Nature* 561, 57–62.
- VanRullen, R., Carlson, T., Cavanagh, P., 2007. The blinking spotlight of attention. *Proc. Natl. Acad. Sci. Unit. States Am.* 104, 19204–19209.
- Vicente, R., et al., 2008. Dynamical relaying can yield zero time lag neuronal synchrony despite long conduction delays. *Proc. Natl. Acad. Sci. U.S.A.* 105, 17157–17162.
- Volgushev, M., et al., 2016. Partial breakdown of input specificity of STDP at individual synapses promotes new learning. *J. Neurosci.* 36 (34), 8842–8855.
- Waldhauser, G.T., Braun, V., Hanslmayr, S., 2016. Episodic memory retrieval functionally relies on very rapid reactivation of sensory information. *J. Neurosci.* 36 (1), 251–260.
- Wimber, M., et al., 2012. Rapid memory reactivation revealed by oscillatory entrainment. *Curr. Biol.* 16 (21), 1482–1486.
- Wyble, B., Bowman, H., Nieuwenstein, M., 2009. The attentional blink provides episodic distinctiveness; sparing at a cost. *J. Exp. Psychol. Hum. Percept. Perform.* 35 (3), 787–807.
- Wyble, B., Potter, M.C., Bowman, H., Nieuwenstein, M., 2011. Attentional episodes in visual perception. *J. Exp. Psychol. Gen.* 140 (3), 488–505.
- Yaffe, R., et al., 2014. Reinstatement of distributed cortical oscillations occurs with precise spatiotemporal dynamics during successful memory retrieval. *Proc. Natl. Acad. Sci. Unit. States Am.* 111 (52), 18727–18732.

Further reading

- Gabor, D., 1946. Theory of communications. *J. Inst Elec Eng* 93, 429–457.
- Gruber, R.W., Klimesch, W., Sauseng, P., Doppelmayr, M., 2005. Alpha phase synchronization predicts P1 and N1 latency and amplitude size. *Cerebr. Cortex* 15, 371–377.
- Henze, D., Buzsáki, G., 2001. Action potential threshold of hippocampal pyramidal cells in vivo is increased by recent spiking activity. *Neuroscience* 105, 121–130.
- Lachaux, J.P., Rodriguez, E., Martinerie, J., Varela, F., 1999. Measuring phase synchrony in brain signals. *Hum. Brain Mapp.* 8, 194–208.
- Schack, B., et al., 2001. Time-variant non-linear phase-coupling analysis of EEG burst patterns in sedated patients during electroencephalographic burst suppression period. *Clin. Neurophysiol.* 112, 1388–1399.